

## II Regional environmental change



## CHAPTER 3

# Tropical oceans

*Jan-Berend W. Stuut, Matthias Prange, Ute Merkel and Silke Steph*

### 3.1 Tropical oceans in the global climate system

The tropical oceans have long been recognised as a key player in global climate as the large gradients in the global heat distribution require strong poleward heat transport out of the tropics through both atmospheric and oceanic processes. A number of oceanic processes make the tropics highly effective in this heat transport; for example the entrainment (upwelling) of cold subsurface waters into the surface layer, which enables the equatorial ocean to absorb atmospheric heat input, and the following transport of these surface waters to the higher latitudes. This process is considered the main balance against the deep-water formation near the poles (e.g. Csanady, 1984). During the past few decades there has been increasing interest in the tropical oceans and their role in global climate throughout the geologic past. As a result, many scientific oceanic expeditions were initiated to study deep-sea sediments, which are thought to have registered such changes in their fossil and sediment content. A number of proxies for oceanic conditions were developed, which will be discussed in section 3.2. As sedimentation rates determine the resolution of the sediment record, deep-sea sediments from the central equatorial basins were used to reconstruct palaeo-oceanographic conditions on longer timescales (millions of years), and records from areas of high-sedimentation rates (e.g.

Amazon and Congo fans) were used for the higher resolved and shorter time spans.

To explore the role of the tropical oceans in global climate we start with the present-day situation in terms of energy balance and consequent oceanic conditions (section 3.1.1) and modern climatologic characteristics like El Niño (3.1.2), forcing factors leading to the observed variability between the ocean basins (3.1.3), the monsoon system (3.1.4) and the role of tropical oceans in the global-ocean circulation (3.1.5). In section 3.2 we discuss the tools currently available to reconstruct palaeoenvironmental conditions, and continue with the state-of-the-art reconstructions of Quaternary climate starting on a glacial–interglacial scale (3.3.1), carrying on with the early Quaternary (3.3.2), through the Mid-Pleistocene Transition (3.3.3) into the late Quaternary (3.3.4), the Last Glacial (3.4.1), the Last Termination (3.4.2) with specific attention for the development of ENSO (3.4.3) and finally the Holocene (3.4.4). The chapter concludes with an outlook of what we have learned from the Quaternary variability in light of future climate scenarios.

#### 3.1.1 Modern climatology

Due to the high amount of solar energy that is received at the low latitudes (see Chapter 1, section 1.1) the upper layer of the tropical oceans is heated, and due to the resulting evaporation its salinity increases (Fig. 3.1). This causes stratification of the

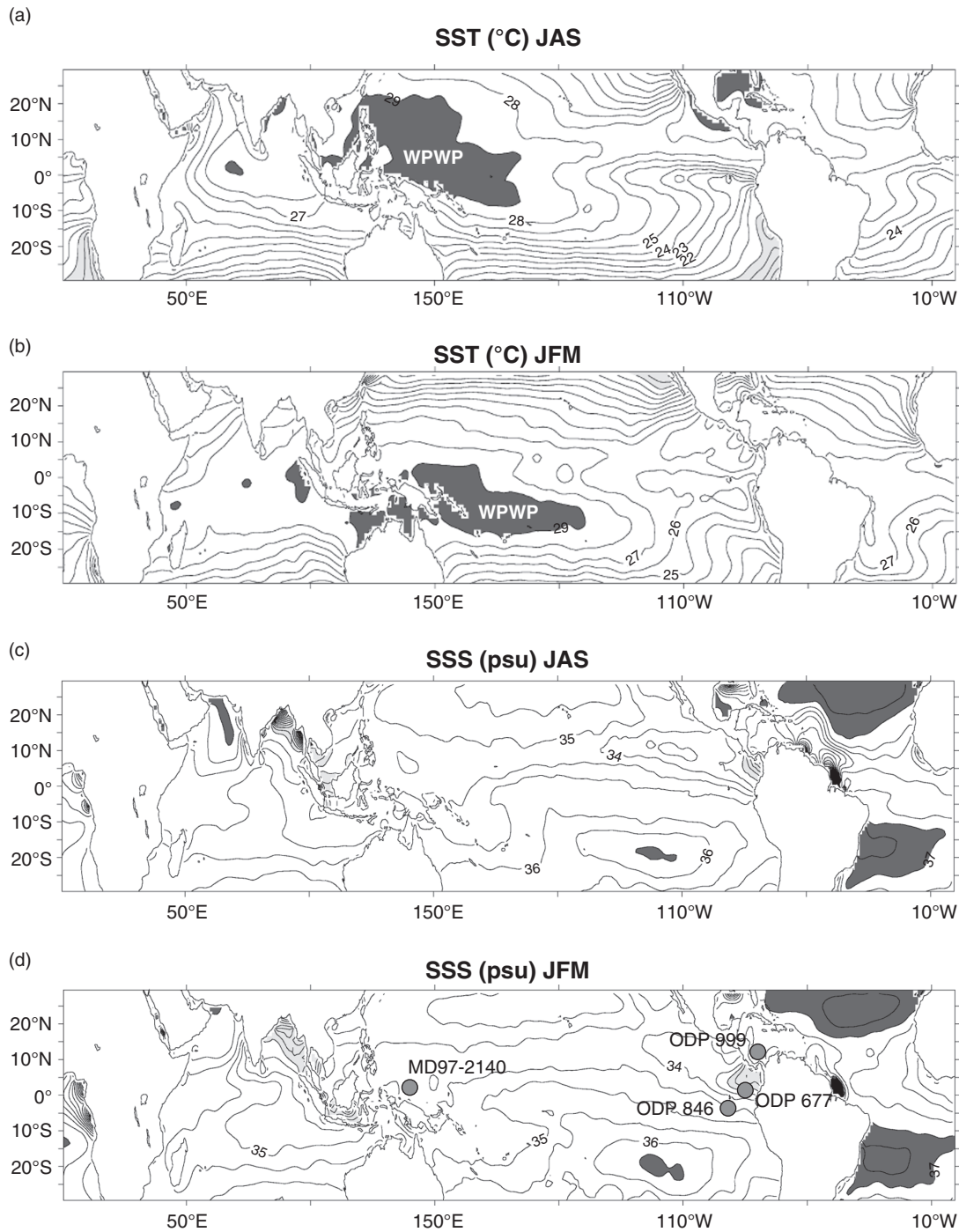


**Fig. 3.1** Present-day summer (July–September; JAS) and winter (January–March; JFM) fields of sea-surface temperature (SST, Figs (a) and (b), contour interval is  $1^{\circ}\text{C}$ ) and sea surface salinity (SSS, Figs (c) and (d), contour interval is  $0.5\text{ psu}$ ). PSU is a dimensionless measure for salinity, according to the practical salinity scale (PSS). Data were taken from the World Ocean Atlas 2005 (Antonov et al., 2006; Locarnini et al., 2006). Grey shadings mark warm pool temperatures ( $>29^{\circ}\text{C}$ , dark grey), cold upwelling regions ( $<18^{\circ}\text{C}$ , light grey), highly net evaporative regions ( $>36.5\text{ psu}$ , dark grey), and distinct fresh regions ( $<33\text{ psu}$ , light grey). The Western Pacific Warm Pool is marked (WPWP). In panel d) the positions of the key sites discussed in this chapter are plotted. (See Colour Plate 3)

tropical ocean with a warm and salty top layer that mixes poorly with the underlying cold deep water. Through the immense energy transfers that take place in the tropical oceans they serve as a heat engine for Earth's climate and as a major moisture source for the Earth's hydrological cycle (Quinn et al., 2006).

As a consequence of such stratification, tropical ocean circulation is primarily in horizontal directions. Following the simplified global ocean conveyor model (Broecker, et al., 1985; see section 3.1.5), net horizontal transport in the tropical Atlantic and Pacific Oceans is northward, while deep waters move southward. The limited vertical exchange that does take place within the low-latitude oceans occurs predominantly in so-called upwelling cells along the eastern continental margins of the Atlantic (e.g. Darbyshire, 1966) and Pacific oceans (e.g. Longhurst, 1967), where denser, colder and nutrient-rich central/mode waters (formed outside the tropics) come to the surface. Upwelling, however, is not restricted to eastern boundary regions. The trade winds induce a transport of water within the wind-driven Ekman layer. Due to the influence of the Coriolis force, the Ekman transport is directed to the right (left) of the surface wind in the Northern (Southern) Hemisphere. This poleward movement of surface waters has to be compensated for by equatorial upwelling bringing cold waters to the surface. This phenomenon is particularly important in the tropical Pacific where a prominent cold tongue of surface waters extends from South America almost to the international dateline, but it is also found in the equatorial Atlantic (e.g. Mitchell and Wallace, 1992; Christian and Murtugudde, 2003). The tropical Pacific and Atlantic mean states are thus characterised by a pronounced east–west gradient in surface and subsurface ocean temperatures. In contrast, there is no evidence of equatorial upwelling in the Indian Ocean (Knauss and Taft, 1963; Tomczak and Godfrey, 2001).

The present-day distribution of sea-surface temperatures (SSTs) in the tropical oceans shows a moderate seasonal variability (Fig. 3.1) with average temperatures of about 18–33 °C. The upwelling areas on the eastern sides of the ocean basins, char-

acterised by low SSTs particularly in Northern Hemisphere summer south of the Equator, are clearly visible. Another striking feature is the lack of seasonal SST variability around the Indonesian archipelago: SSTs are year-round warmer than 28 °C. Because of these continuously high temperatures, the region is called the Western Pacific Warm Pool (WPWP), which contributes explicitly to the global heat engine (e.g. Quinn et al., 2006).

The sea surface salinity (SSS) map of the tropical oceans (Fig. 3.1) illustrates that despite the high SSTs, the WPWP is characterised by relatively fresh waters, resulting from excessive tropical rainfall and river runoff in this area. Moreover, freshwater plumes are visible off major rivers including the Ganges-Brahmaputra in East Asia, the Niger and Congo in Africa, and the Amazon in northeastern South America. The low-salinity pool in the tropical eastern Pacific can be attributed to atmospheric moisture fluxes from the Atlantic to the Pacific across the Central American Isthmus as well as to westerly moisture transport from the central Pacific to the Panama Bight (e.g. Prange et al., 2010). Extremely high salinities are observed in semi-enclosed basins like the Red Sea and Arabian Gulf, where evaporation is high (>5 m/a) and river runoff is limited.

Upwelling of cold subsurface waters on the eastern side of the oceans is primarily driven by tropical trade winds that drive a westward flow of warm surface waters. As a consequence, these warm waters pile up against the eastern margins of the continents on the western sides of the Pacific and Atlantic Oceans. In the Indian Ocean the reverse is observed; SSTs at the western side of the basin are lower than those in the east, which is due to the strong seasonal monsoon-driven upwelling along the east African coast (e.g. Webster et al., 1999). Upwelling of cold and nutrient-rich subsurface waters boost the primary productivity in these areas and, as a consequence, past variability in upwelling intensity and hence the strength of the monsoon is often reconstructed from past variability in primary productivity (e.g. Schulz et al., 1998; Beaufort et al., 2001; Wang et al., 2005).

The performance of state-of-the-art general circulation models of the coupled ocean–atmosphere

system in representing the tropical oceans' mean state and variability has been addressed in several international projects. Whilst the El Niño Simulation Intercomparison Project (ENSIP; Latif et al., 2001) focused on the tropical Pacific, all tropical oceans were addressed in the Study of Tropical Oceans In Coupled General Circulation Models (STOIC) project (Davey et al., 2002). These studies demonstrate the ability of general circulation models to represent interannual variability, but also document the shortcomings in simulating correctly the ocean mean state, such as the zonal SST distribution in equatorial regions. More recent studies, such as the detailed intercomparison by Guilyardi (2006), emphasise the progress of a significant number of general circulation models in correctly reproducing the main features of equatorial climate, in particular SST.

### 3.1.2 El Niño–Southern Oscillation and its relatives

Tropical Pacific variability is mostly explained by the annual cycle and the interannual variations related to the El Niño–Southern Oscillation (ENSO, see also Chapter 2, section 2.5.1, and Chapter 9, section 9.4.1). ENSO is the most prominent phenomenon of interannual climate variability. During El Niño episodes, the upwelling of cold and nutrient-rich water in the eastern tropical Pacific is strongly reduced. This leads to a large-scale warming of the upper layers of the tropical Pacific, with considerable SST anomalies of up to 5°C near the west coast of South America. By contrast, La Niña episodes exhibit anomalously low ocean surface temperatures due to enhanced equatorial and coastal upwelling in the eastern Pacific. ENSO is a prominent example of the close interaction between the ocean and the atmosphere. Coupled to SST variations, the contrast in sea-level pressure across the tropical Pacific also exhibits temporal variations ('Southern Oscillation'), which become manifest in the strength of the trade winds. During El Niño, the trade winds are weakened, whereas during La Niña, an intensification of the trade winds is observed. The positive ocean–atmosphere feedback during the development of an El Niño (La Niña) event was first described by Bjerknes (1969).

It should be noted that the observed distribution of SST anomalies (e.g. for the widely used Niño-3 diagnostic, a box-average for the eastern tropical Pacific; 150°W–90°W, 5°S–5°N) is skewed towards El Niño events, that is warm events tend to exhibit a stronger amplitude than cold events (see Trenberth, 1997).

The ENSO phenomenon induces a major reorganisation of the atmospheric circulation. The major convection zones are shifted from the WPWP towards the east; Indonesia and northern Australia usually experience a substantial decrease in precipitation while wetter conditions are observed over western South America. As noted by Tribbia (1991), however, the oceanic ENSO changes and the concomitant reorganisation of the atmospheric circulation exhibit a clear disparity in scale. Via teleconnections, the tropical Pacific anomalies are communicated to regions beyond the tropical Pacific realm (Trenberth et al., 1998; Alexander et al., 2002). These provide the ENSO phenomenon with a socio-economic dimension (Pielke Jr. and Landsea, 1999; Laosuthi and Selover, 2007) through the impacts on fishery along the South American coast, on the pricing of agricultural products (e.g. coconut oil, rice), and on national economies through damage induced by Atlantic hurricanes which are found to be more frequent during La Niña seasons (Pielke Jr. and Landsea, 1999). Therefore, an accurate prediction of ENSO is not only of scientific interest but also of economic and political relevance. Much progress has been achieved in predicting ENSO through the setup of the observational TOGA/TAO buoy array in the tropical Pacific and altimeter data of sea-level height becoming available from satellites, and through the assimilation of these products into seasonal forecasting systems which leads to considerably better forecasting skill (Latif et al., 1998).

In addition to the annual cycle and ENSO, there is also evidence that sub-ENSO variability on timescales of 1–2 years provides a significant contribution to tropical Pacific variability (e.g. Jin et al., 2003; Keenlyside et al., 2007). On longer timescales, ENSO may also be modulated by the subtropical north and south Pacific oceans or exhibit a coupling to mid latitude decadal

variability (Trenberth and Hurrell, 1994; Schneider et al., 1999; Matei et al., 2008).

Tropical Atlantic interannual variability is mostly described by two modes. The equatorial mode (Zebiak, 1993) bears some resemblance to its Pacific counterpart, ENSO. Furthermore, a meridional mode (Chang et al., 1997; Servain et al., 1999), which involves meridional displacements of the Intertropical Convergence Zone (ITCZ) and an interhemispheric gradient of SST, contribute to Atlantic variability. The meridional mode and the equatorial mode seem to be coupled on interannual and decadal timescales. In addition, the Atlantic is not completely decoupled from the tropical Pacific (Enfield and Mayer, 1997; Chang et al., 2006). In the Indian Ocean, a pattern of internal variability with anomalously low (high) SSTs off Sumatra and high (low) SSTs in the western Indian Ocean has been identified (Saji et al., 1999). This so-called Indian Ocean Dipole can cause severe rainfall in eastern Africa and droughts in Indonesia, and may even affect the strength of the Indian summer monsoon (Ashok et al., 2001).

### 3.1.3 Solar and volcanic radiative forcing of tropical oceans

It has been suggested that ENSO-like events can be induced by external forcings associated with explosive tropical volcanic eruptions or variations in solar activity (Mann et al., 2005). The underlying mechanism can be described as an ‘ocean dynamical thermostat’ in which an anomalous heating of the tropical Pacific results in a cooling of the eastern part of the basin, that is La Niña-like conditions (Clement et al., 1996). Briefly, the mechanism works as follows: in the western equatorial Pacific, where the thermocline is deep, the response of the mixed layer to a surface heating is largely thermodynamic, leading to a rise in SST. In the eastern equatorial Pacific, where the thermocline is shallow, the surface heating is offset by vertical advection of cool water, leading to a smaller SST response than in the western part of the basin. As a result, the zonal SST gradient increases, leading to stronger trade winds and further thermocline shoaling and cooling by vertical advection in the east, further strengthening of the trades, and so on. This feed-

back, akin to the Bjerknes feedback that operates on interannual timescales, results in a cooling of the eastern equatorial Pacific in response to heating of the basin. Although this mechanism is basically a pure theoretical construct which ignores possibly important feedbacks (e.g. cloud radiative feedbacks) there seems to be some observational evidence that supports the notion of this ‘dynamical thermostat’ on the multidecadal-centennial (Mann, et al., 2005 and references therein) and millennial (Marchitto et al., 2010) timescales. Moreover, this mechanism could help to explain apparent evidence that extra-tropical temperature changes in past centuries were greater in amplitude than tropical ones (cf. Esper et al., 2002; Hendy et al., 2002).

A completely different mechanism has been suggested by Meehl et al. (2003). They suggest that the tropical Pacific Ocean may act as an amplifier for extra-tropical climate change in response to relatively weak changes in total solar irradiance. The authors describe the following coupled air–sea response mechanism to solar forcing over the Pacific: over relatively cloud-free oceanic regions in the subtropical areas of low-level moisture divergence, enhanced solar irradiance causes greater evaporation. As a result, more moisture is advected by the trade winds into the tropical precipitation zones (areas of low-level moisture convergence), enhancing rainfall and intensifying the upward motions of the regional Hadley and Walker circulations. The enhanced subsidence (over areas of low-level moisture divergence) associated with the intensified regional vertical motion further reduces the cloudiness over the subtropical ocean regions, allowing even more solar radiation to reach the surface, and so on (Fig. 3.2). The strengthening of the trade winds (associated with intensification of the Hadley and Walker circulations) results in greater upwelling of colder water and a westward extension of the equatorial Pacific cold tongue. This reduces rainfall across the equatorial Pacific, while precipitation increases in the Pacific ITCZ and the South Pacific Convergence Zone (Meehl et al., 2008).

Experiments with an atmosphere general circulation model showed that mid-tropospheric heating anomalies associated with tropical rainfall changes

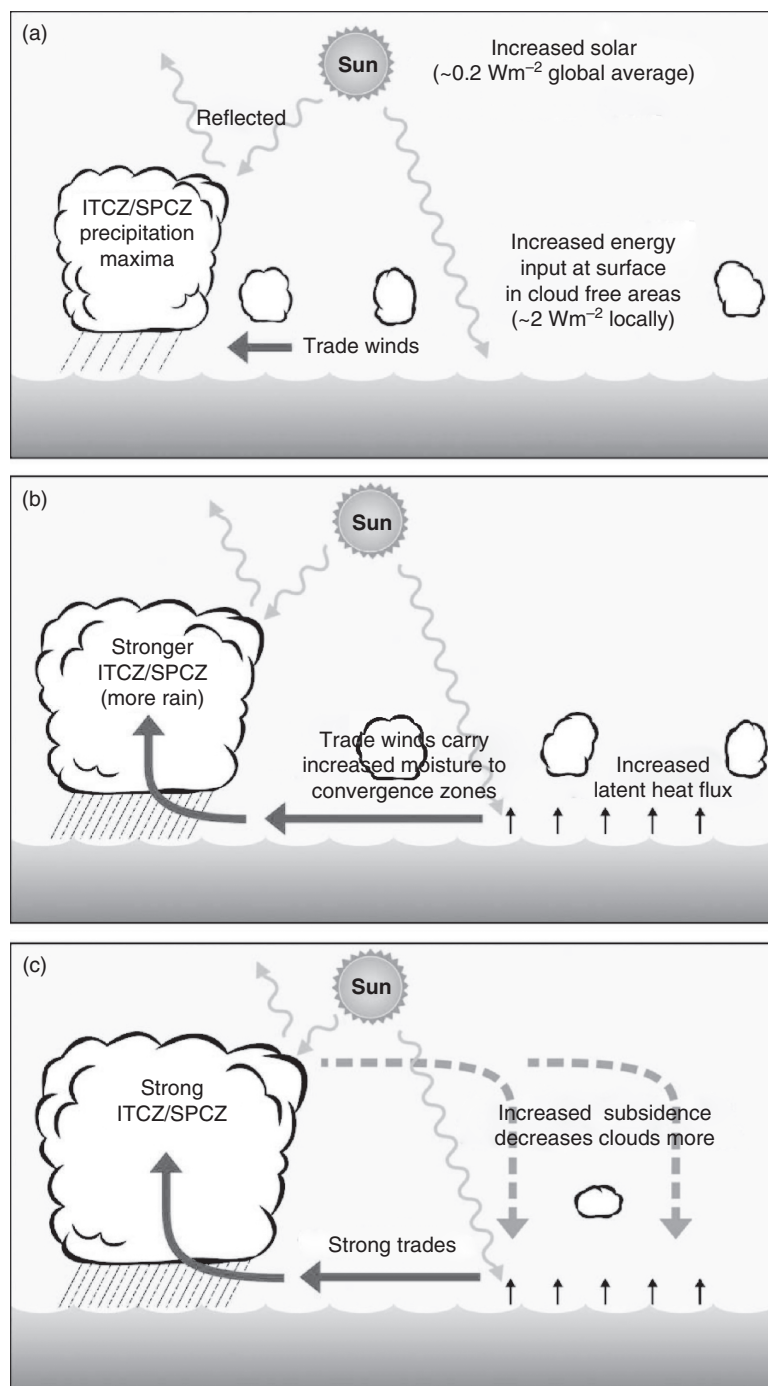


**Fig. 3.2** Diagram depicting the coupled air-sea response mechanism to solar forcing over the Pacific as suggested by Meehl et al. (2003, 2008). The feedback loop involves changes in latent heat fluxes at the subtropical ocean surface, the intensity of the Walker and Hadley circulations, tropical rainfall and subtropical low clouds (from Meehl et al., 2008). © American Meteorological Society. Reprinted with permission.

result in an anomalous Rossby wave response in the atmosphere and consequent positive sea-level pressure anomalies in the north Pacific extending to western North America and even influencing the Arctic Oscillation (Meehl et al., 2008). These experiments suggest that the tropical oceans are not only subject to important feedback mechanisms but that they also strongly impact on extra-tropical climate.

### 3.1.4 Tropical oceans and monsoons

During the last few years, attention has shifted to the tropical oceans and monsoon systems (African, Asian and South American) as an important link in the global ocean circulation through their heat and freshwater budgets. Changes in the hydrological cycle (evaporation versus precipitation and runoff causing salinity changes in the surface waters) obviously are a key link in the global ocean circulation. During the Quaternary, the African and Indian monsoons (Prell and Kutzbach, 1992) as well as the East Asian monsoon (Wang et al., 2005) have been shown to have been tied to Northern Hemisphere insolation, varying in pace with precession and obliquity forcing. In most studies, the monsoon has been considered as one phenomenon affecting a tropical belt from Africa across India into East Asia. Recently, it has been shown that there are differences in the responses of the different monsoon subsystems to orbital forcing and in the seasonal timing of insolation forcing (Braconnot, et al., 2008). Such differences encompass, for example, feedbacks from the tropical ocean that tend to amplify the insolation-induced African monsoon, whereas the same feedbacks tended to weaken the Indian monsoon during the mid Holocene (Braconnot et al., 2007a,b). Instrumental data indicate the substantial role of tropical ocean SSTs in driving the West African monsoon (Giannini et al., 2003).

### 3.1.5 The tropical oceans as part of the global conveyor belt

As there were only minor changes in the tectonic configuration of the global ocean basins throughout the Quaternary, it is assumed that the now well-established concept of the global ocean circulation (Wüst, 1935; Stommel et al., 1956) operating

as the 'Great Ocean Conveyor' (Broecker, 1991) acted in basically the same way as today (Fig. 3.3).

The general, simplified picture of the global ocean circulation contains a wind-driven upper ocean circulation with strong surface currents like the Gulf Stream in the Atlantic, and the Kuroshio and Humboldt currents in the Pacific Ocean. Superimposed on this surface circulation there is a thermohaline circulation, which basically encompasses heat and salt-driven density currents. Surface currents head northward from the equatorial Atlantic Ocean, cooling on their way and eventually sinking in the North Atlantic and the Nordic Seas. This dense and cold water then flows southward in a deep Atlantic western boundary current and – via the Antarctic Circumpolar Current – into the Indian and Pacific oceans. The major part of these cold and dense deep waters upwells in the Southern Ocean due to diapycnal mixing and Ekman pumping, where the waters may cool even further and hence may be shed back northward at depth into the three ocean basins. The oldest water masses (~2000 years radiocarbon age) in the world ocean are found in the North Pacific below 1500 m (Östlund and Stuiver, 1980). The upper-ocean return flow to the North Atlantic occurs via two different paths. Along the surface of the Pacific Ocean, through the Indonesian Archipelago and Indian Ocean, waters that gradually warm up and become salty along their path at the surface of the oceans re-enter the Atlantic Ocean with the Agulhas Current south of South Africa ('warm-water path'). The other path goes from the Pacific to the Atlantic via the Drake Passage between South America and Antarctica ('cold-water path').

The global redistribution of heat and salt can be interrupted when changes occur anywhere along its route. For example, the global conveyor can be decelerated when the high-saline inflow from the Indian into the Atlantic Ocean, south of Africa, is hampered or completely blocked, as was shown to have happened occasionally throughout the late Quaternary (Peeters et al., 2004). Alternatively, if additional fresh water is added into the North Atlantic, waters may not become sufficiently dense to sink and the global conveyor slows down. Indeed, large armadas of icebergs

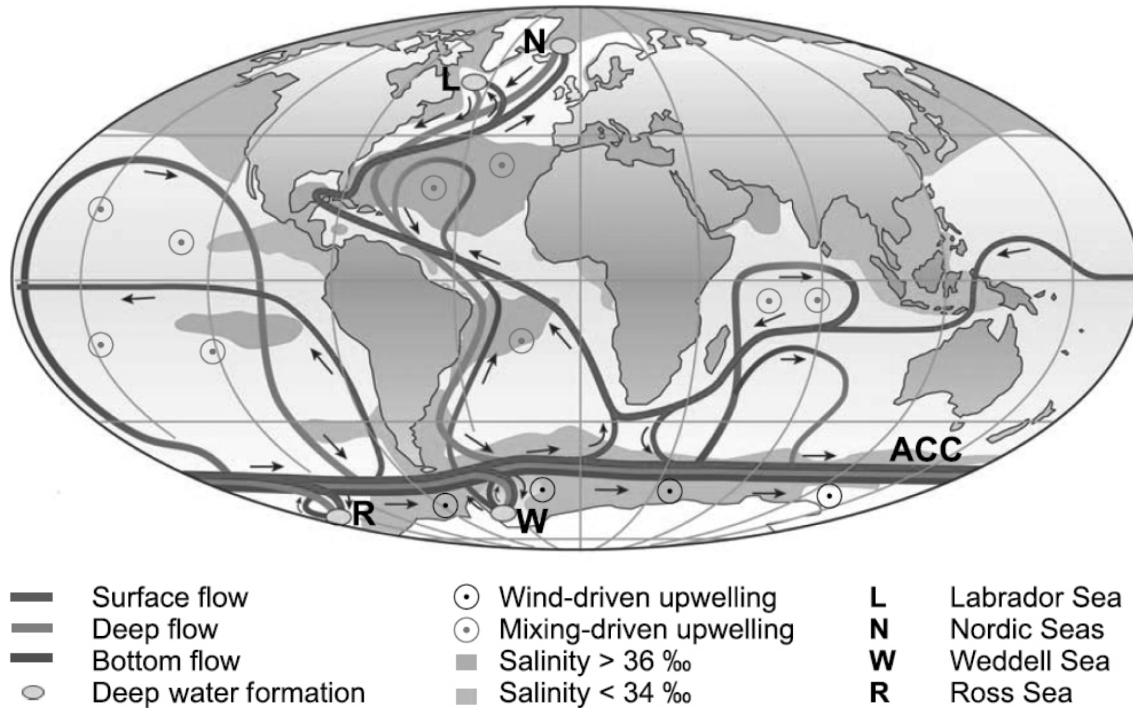


**Fig. 3.3** The wind-, heat-, and salt-driven global ocean conveyor. Deep currents are light grey, surface currents are dark grey. Warm and salty waters in the Atlantic Gulf Stream move along the surface towards the north where they are cooled and sink to the bottom. In the deep Atlantic Ocean they move southward and after flowing along the Antarctic Circumpolar Current they are distributed into the Indian and Pacific Oceans. The return flow is along the surface of the Pacific and Indian Oceans towards the South and into the Atlantic Ocean (from Kuhlbrodt et al., 2007). © (2011) American Geophysical Union. Reproduced by permission of American Geophysical Union. (See Colour Plate 4)

drifting into the North Atlantic during so-called Heinrich Events, which characterise the late Quaternary, injected huge amounts of meltwater into the North Atlantic and consequently slowed down the global ocean conveyor (Bond et al., 1992). As a consequence of the interrupted northward oceanic heat transport, the Northern Hemisphere cooled dramatically, while the Southern Hemisphere experienced millennial-scale warming (the so-called ‘bipolar seesaw’). We note, however, that there is still no consensus on the actual cause of Heinrich Events or the higher-frequency Dansgaard–Oeschger Events, which are characteristic of Marine Isotope Stage 3, but it has been hypothesised that both also occurred during the geologic past before 60 kyr BP (e.g. Eyles et al., 1997). Another drastic perturbation of the ocean

circulation occurred during the Younger Dryas stadal (c. 12.8 to 11.5 kyr BP). It has been hypothesised that this cold event was caused by the abrupt release of floodwater from Megalake Agassiz in eastern North America. This gigantic release of freshwater into the North Atlantic caused the global ocean conveyor to slow down, similar to the Heinrich Events (Broecker et al., 1989; Lowell et al., 2005). Modelling studies have shown that such a cause (freshwater pulses) and effect (slowdown of the global ocean conveyor) is realistic (see Chapter 9, section 9.4.3) and can lead to temperature and moisture effects that are recorded globally (Ganopolski and Rahmstorf, 2001; Prange et al., 2004). Through both oceanic and atmospheric teleconnections, perturbations of the thermohaline conveyor had a dramatic impact

on the tropical hydrologic cycle (Mulitza et al., 2008; Tjallingii et al., 2008; Collins et al., 2011).

## 3.2 Reconstructing past ocean conditions

### 3.2.1 Proxies for SST and SSS

SST and SSS are key variables for reconstructing past changes in climate and ocean circulation, and provide important clues for climate modelling (see also Chapter 9, section 9.2.3). Therefore, they are of major interest in palaeoceanographic studies. A large number of proxies are available to assess past changes in SST (Table 3.1) and SSS. Assemblage counts of calcareous or siliceous microplankton, geochemical proxies such as the stable oxygen isotopic composition and Mg/Ca ratios in planktonic foraminiferal calcite shells and unsaturation ratios of long-chain alkenones from haptophyte algae are among the most commonly used.

**Table 3.1** Major proxies for past SST determinations.

Proxy	Applicable to	Reference papers
$\delta^{18}\text{O}$	Carbonates (e.g. foraminifera, shells)	(Urey, 1947; McCrea, 1950; Epstein et al., 1953; Shackleton, 1974;)
Faunal transfer functions	Foraminifera, Radiolaria etc.	(Imbrie and Kipp, 1971; Pisias and Mix, 1997)
$\text{U}_{37}^{\text{K}}$ , $\text{U}_{37}^{\text{C}}$	Alkenones in haptophyte algae	(Brassell et al., 1986; Prah and Wakeham, 1987; Müller et al., 1998)
Sr/Ca ratios	Corals	(Beck et al., 1992)
Mg/Ca ratios	Planktonic foraminifera	(Nürnberg et al., 1996; Lea et al., 1999; Elderfield and Ganssen, 2000)
Ca isotopes	Carbonates (e.g. forams, shells, corals)	(Zhu and Macdougall, 1998; Nägler et al., 2000)
$\text{TEX}_{86}$	Lipids in cell membrane	(Schouten et al., 2002)

Analyses of stable oxygen isotopes in foraminiferal calcite tests have played a pivotal role in palaeoceanography since the 1950s, when Emiliani (1955) first interpreted the oxygen isotopic record from deep-sea cores to reflect a series of Pleistocene climate/temperature cycles. The oxygen isotopic composition of calcite ( $\delta^{18}\text{O}$ ) is determined by comparing oxygen isotope ratios ( $^{18}\text{O}/^{16}\text{O}$ ) of the measured samples with the  $^{18}\text{O}/^{16}\text{O}$  ratio of an external standard, and is defined as:

$$\delta^{18}\text{O}_{\text{sample}}(\text{‰}) = \left[ \frac{(^{18}\text{O}/^{16}\text{O})_{\text{sample}} - (^{18}\text{O}/^{16}\text{O})_{\text{standard}}}{(^{18}\text{O}/^{16}\text{O})_{\text{standard}}} \right] * 1000$$

' $\delta^{18}\text{O}$  palaeo-thermometers' or ' $\delta^{18}\text{O}$ -temperature equations' applied to convert measured  $\delta^{18}\text{O}_{\text{calcite}}$  into water temperatures are based on the thermodynamic fractionation of  $^{16}\text{O}$  and  $^{18}\text{O}$  between water and newly formed carbonate, which results in about 0.20–0.27‰ depletion in  $\delta^{18}\text{O}_{\text{calcite}}$  for every 1°C temperature increase (Urey, 1947; Epstein et al., 1953; O'Neil et al., 1969; Shackleton, 1974; Erez and Luz, 1983; Kim and O'Neil, 1997; Bemis et al., 1998; Zhou and Zheng, 2003). Yet  $\delta^{18}\text{O}_{\text{calcite}}$  also depends on the oxygen isotopic composition of the seawater from which the carbonate precipitated ( $\delta^{18}\text{O}_{\text{seawater}}$ ).  $\delta^{18}\text{O}_{\text{seawater}}$  is intimately linked with fractionation processes within the hydrological cycle; water molecules composed of lighter isotopes ( $^{16}\text{O}$ ) have higher vapour pressures and are thus preferentially enriched in the vapour phase.

Seawater  $\delta^{18}\text{O}$  is basically a measure for changes in global ice volume (mean ocean  $\delta^{18}\text{O}$ ) as well as for local variations in the oxygen isotopic composition of seawater. If the amount of continental ice increases (e.g. during glacials), the long-term storage of isotopically light water within the ice sheets affects the global  $\delta^{18}\text{O}$  balance by leaving the global ocean enriched in  $^{18}\text{O}$ . In contrast, the melting of ice sheets supplies  $^{16}\text{O}$ -enriched water to the ocean and accordingly lowers global-ocean  $\delta^{18}\text{O}$  (e.g. Shackleton, 1987; Fairbanks, 1989; Schrag et al., 1996; Waelbroeck et al., 2002). Local changes in the oxygen-isotopic composition of surface water are driven by changes in freshwater supply via precipitation directly onto the sea surface or via river

runoff, and by variations in the  $\delta^{18}\text{O}$  of atmospheric vapour. Arid, evaporative regions demonstrate surface water  $\delta^{18}\text{O}$  enrichment, whereas areas of high precipitation or those in close proximity to a river mouth are affected by the (relatively low) average  $\delta^{18}\text{O}$  of precipitation over the sea surface or over the river's catchment area. The oxygen-isotopic fractionation of water during evaporation/precipitation therefore also links  $\delta^{18}\text{O}_{\text{seawater}}$  to salinity. On average,  $\delta^{18}\text{O}_{\text{seawater}}$  increases by approximately 0.5‰ per practical salinity unit (psu; Broecker, 1989), although  $\delta^{18}\text{O}_{\text{seawater}}$ -salinity relationships can be subject to strong local and temporal variations due to the varying isotopic composition of freshwater (e.g. Fairbanks et al., 1992; Schmidt et al., 2001).  $\delta^{18}\text{O}$  of planktonic foraminiferal calcite can thus serve not only as a temperature proxy but also as a measure of local changes in salinity, if the temperature signal is determined independently and extracted from the measured  $\delta^{18}\text{O}$  record (i.e. using Mg/Ca-based temperature reconstructions). Additional prerequisites are that corrections for temporal changes in global ice volume are applied (e.g. Waelbroeck et al., 2002), and that suitable  $\delta^{18}\text{O}_{\text{seawater}}$ -salinity relationships are available for the study area.

Since the late 1990s, the ratio between Magnesium and Calcium in foraminiferal calcite tests has been established as a proxy for past changes in water temperature. The underlying basis for Mg/Ca palaeothermometry is that the substitution of magnesium in calcite is endothermic and therefore is favoured at high temperatures. Numerous calibration studies have shown that Mg/Ca ratios in the calcite tests of several planktonic foraminiferal species increase exponentially with increasing water temperature, whereas the incorporation of  $\text{Mg}^{2+}$  into foraminiferal tests is probably partly biologically mediated (e.g. Nürnberg et al., 1996; Lea et al., 1999; Mashiotto et al., 1999; Elderfield and Ganssen, 2000; Dekens et al., 2002; Anand et al., 2003; Regenberg et al., 2009).

Sr/Ca ratios in corals were also shown to provide a promising proxy for water temperature variability (Beck et al., 1992; Felis and Pätzold, 2004). Although there are differences in temperature calibrations between different studies, the average Sr/

Ca SST calibration suggests a temperature dependence of 0.062 mmol/mol per 1°C. Recent studies revealed that U/Ca ratios in corals could provide a temperature proxy of comparable accuracy (Corrège et al., 2000).

Another geochemical proxy commonly used for SST reconstructions is based on an organic biomarker: the unsaturated ratios in long-chain alkenones produced by single-celled haptophyte algae that dwell near the sea surface ( $\text{U}^{\text{K}}_{37}$  index or  $\text{U}^{\text{K}}_{37}$  index; Brassell et al. 1986; Prahl and Wakeham 1987). Major alkenone producers in the modern marine environment are the coccolithophores *Emiliania huxleyi* and *Gephyrocapsa oceanica*. They respond to changes in ambient water temperature by altering the number of double bonds (two, three or four) in their unsaturated alkenones, which are then preserved in marine sediment records (Prahl and Wakeham, 1987). The currently accepted  $\text{U}^{\text{K}}_{37}$  index is defined by the ratio between di-unsaturated alkenones and the sum of di- and tri-unsaturated alkenones, and varies positively with temperature. The  $\text{TEX}_{86}$  proxy (Schouten et al., 2002), which is based on glycerol dialkyl glycerol tetraethers (GDGTs) produced by Marine Group I Crenarchaeota, is usually thought to reflect SST. However, recent studies suggest that  $\text{TEX}_{86}$  may rather reflect subsurface temperatures in certain regions, since Crenarchaeota can reside deeper in the water column and are not restricted to the photic zone (e.g. Hugué et al., 2007; Lopes dos Santos et al., 2010).

A relatively new hydrologic proxy is based on the hydrogen isotopic composition of the long-chain alkenones produced by haptophyte algae ( $\delta\text{D}$ ). Like oxygen, hydrogen plays a dominant role in the hydrological cycle. Similar to the fractionation of oxygen isotopes during evaporation, the hydrogen isotopic ratio of water vapour is depleted in deuterium owing to the lower vapour pressure of DHO compared to  $\text{H}_2\text{O}$  (Craig, 1961). Evaporation thus leads to a relative D depletion of precipitation and D enrichment of lake- and seawater. In the tropics, changes in seawater  $\delta\text{D}$  are mainly controlled by changes in the amount of local precipitation and river runoff to the ocean, whereas the temperature-dependent fractionation of hydrogen isotopes is

close to zero at low latitudes (e.g. Rozanski et al., 1992). Culturing experiments have shown that long-chain alkenones produced by haptophyte algae reflect  $\delta D$  of the water in which the alkenones were produced with near perfection (although with a negative offset due to isotope fractionation during alkenone synthesis; Paul, 2002; Englebrecht and Sachs, 2005; Schouten et al., 2006).  $\delta D$  measured in alkenones from marine sediments thus provides a promising tool to reconstruct past changes in freshwater supply to the ocean by precipitation and river runoff.

### 3.2.2 Reconstructing continental climate using marine archives

In addition to oceanic conditions, environmental changes on land can be reconstructed from the terrigenous sediment fraction of marine sediments (e.g. Prins and Weltje 1999; Stuut et al., 2002, 2004, 2007; Frenz et al., 2003; Stuut and Lamy, 2004; Collins et al., 2011; Meyer et al., 2011). Potentially, reconstructions of past oceanographic conditions can be combined with reconstructions of environmental conditions on land, ideally from the same sediment cores, leading to conceptual models of natural climate change. Following this approach for the continents on the Southern Hemisphere, it was shown that the winter rains, related to the latitudinal variability of the southern westerlies, had a strong influence on regional climates in Chile and South Africa on a glacial–interglacial scale, most likely driven by variability in Antarctic sea-ice extent (Stuut et al., 2004; Stuut and Lamy, 2004). Further, sediments on the northwestern African continental slope were demonstrated to be mixtures of river-transported material and wind-blown dust (Holz, et al., 2004, 2007; Stuut et al., 2005). Using an end-member approach (Weltje, 1997) it is possible to numerically deconvolve this mixture into a limited number of subpopulations, consequently interpreted as fluvial mud and aeolian dust, respectively, which can be quantified down-core. In this way, it was suggested that changes in the overturning circulation in the North Atlantic Ocean caused abrupt and lasting periods of aridity in the Sahel contemporaneous with Heinrich Events (Mulitza et al., 2008; Niedermeyer et al.,

2009; Tjallingii et al., 2008; Zarris et al., 2011). Finally, following the same approach it was demonstrated that natural climate variability was strongly overprinted by anthropogenic agricultural activities, which has led to an increase in dust emissions in northwestern Africa during the past few centuries (McGregor et al., 2009; Mulitza et al., 2010).

## 3.3 Tropical oceans throughout the Quaternary

### 3.3.1 Glacial–interglacial cycles

As insolation has varied throughout the Quaternary as a consequence of the changing position and distance of the Earth relative to the Sun (Milankovitch, 1941), so the resulting SSTs and ocean currents have not been constant through time. Throughout the Quaternary, the climate of the Earth has been characterised by a succession of about 50 glacial–interglacial cycles (Fig. 3.4), which are ultimately attributed to insolation changes (e.g. Shackleton et al., 1990). However, internal feedbacks involving atmospheric  $CO_2$ , ice albedo, and dust had a major influence on the distribution of energy (e.g. Ruddiman, 2006). The first record from a tropical ocean that resolved about 12 Quaternary glacial–interglacial cycles was published by Shackleton and Opdyke (1973) who constructed a 870-kyr stable oxygen isotope record from a sediment core from the equatorial Pacific. Later, this proxy was used not only to date other sediment records, but also to extend the geological timescale (e.g. Shackleton et al., 1990). In the following paragraphs the characteristic changes and their driving mechanisms are discussed for different distinct periods throughout the Quaternary.

### 3.3.2 Early Quaternary (the ‘41-kyr world’)

During the early Quaternary, Milankovitch-type climate variability was shown to have been dominated by obliquity (variations in the tilt of the Earth’s rotational axis), leading to relatively short-term (~41 kyr) variations. This allowed the growth

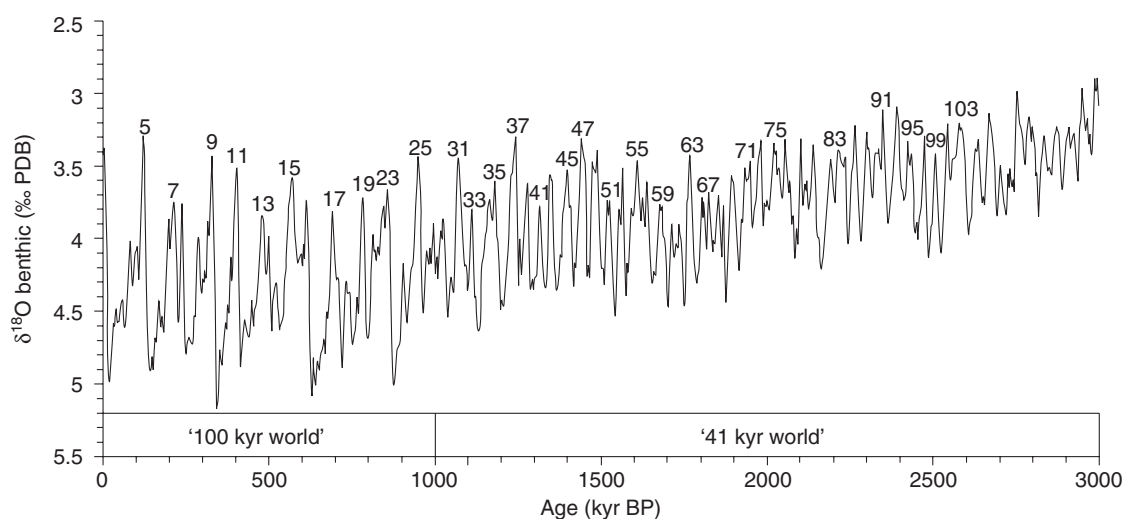


**Fig. 3.4** Quaternary composite benthic  $\delta^{18}\text{O}$  record from the equatorial Pacific (ODP Site 677; Shackleton et al., 1990). Marine Isotope Stages are indicated for the interglacial periods. Data are from: Shackleton, N. (1996) Timescale Calibration, ODP 677. IGBP PAGES/World Data Center-A for Paleoclimatology Data Contribution Series # 96-018. NOAA/NGDC Paleoclimatology Program, Boulder CO, USA.

of only relatively small ice sheets at the poles during glacial intervals, but possibly also resulted in larger residual polar ice caps during interglacials (e.g. Prell, 1982). Consequently, the amplitude of glacial–interglacial cycles was relatively small.

Low-resolution studies on benthic Mg/Ca suggest that, after a long-term cooling of the deep ocean through the Pliocene, the early Pleistocene witnessed a return to higher Mg/Ca ratios that is not apparent in the oxygen isotope record (Billups and Schrag, 2002). This temperature effect has not been calculated yet on the glacial–interglacial timescale. By contrast, there is evidence from the eastern tropical Pacific that SST during the early Quaternary was somewhat warmer than today, gradually cooling down over the course of the early Quaternary (Fig. 3.5). Tropical SST variability was dominated by approximately 41 kyr obliquity cycles, which are characteristic for the high latitudes (Liu and Herbert, 2004). The processes leading to the transmission and amplification of the obliquity signal from high to low latitudes remain unclear (de Garidel-Thoron, 2007).

### 3.3.3 Mid-Pleistocene Transition

At some point during the early–mid Pleistocene there was a shift from obliquity-dominated (~41 kyr) to eccentricity-dominated (~100 kyr) climate variability (see Fig. 3.4), modulated by precession (19–23 kyr) (see Chapter 1, section 1.4). This so-called Mid-Pleistocene Transition (MPT) or Revolution began 1.25 Ma BP and was complete by about 650 kyr BP (e.g. Tziperman and Gildor, 2003; Schefuß et al., 2004; Medina-Elizalde and Lea, 2005; Clark et al., 2006). Its onset was accompanied by decreases in North Atlantic SSTs as well as by increased African and Asian aridity. In the obliquity-dominated world prior to the transition, the response of the global climate system to orbital-insolation changes was rather linear, resulting in distinctive sinusoidal  $\delta^{18}\text{O}$  records varying in concert with insolation (Imbrie et al., 1992). After the transition, both the amplitude of changes and the temporal response of the global ocean increased dramatically, resulting in the so-called saw-tooth shape of late Pleistocene ice-volume changes (Imbrie et al., 1993), with relatively slow glaciations

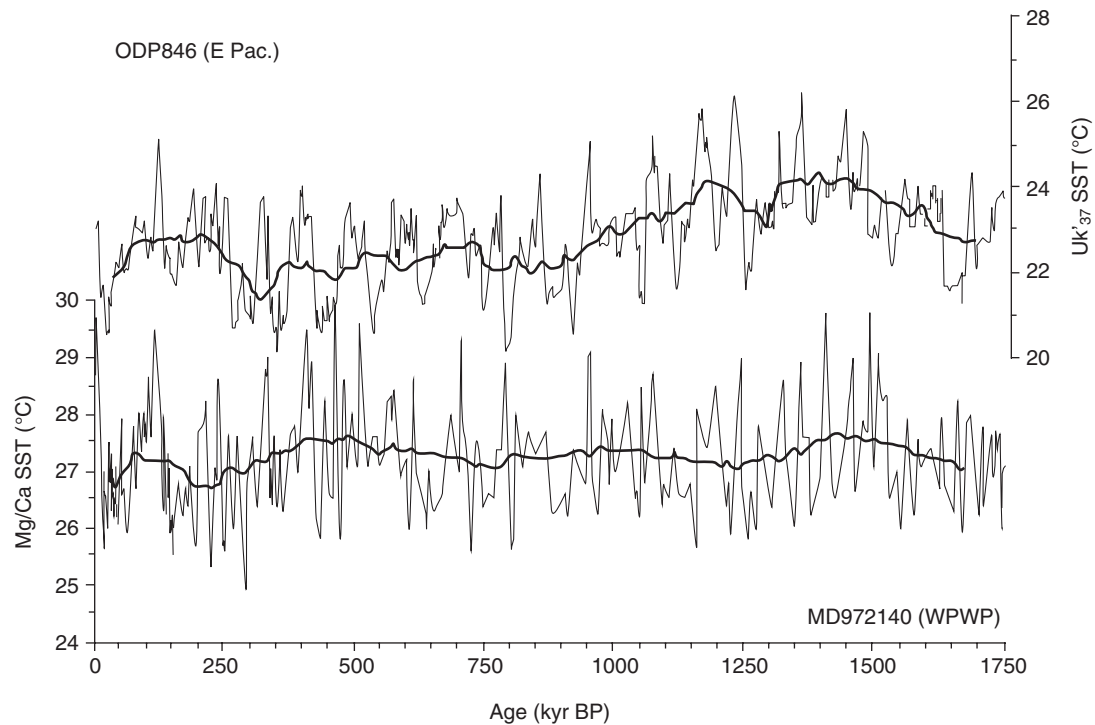


**Fig. 3.5** Quaternary SST comparison between western (de Garidel-Thoron et al., 2005) and eastern (Lawrence et al., 2006) tropical Pacific records.

and rapid deglaciations. The MPT shift from approximately 41 to approximately 100 kyr dominant variability is clearly visible in tropical SST records (de Garidel-Thoron et al., 2005; Medina-Elizalde and Lea, 2005).

On the eastern (upwelling) side of both the tropical Atlantic (Marlow et al., 2000), and the tropical Pacific (Lawrence et al., 2006) ocean surface temperatures gradually decreased during the early Pleistocene before the MPT. However, temperatures outside the upwelling region in the Atlantic (Schefuß et al., 2004) and in the western part of the tropical Pacific (de Garidel-Thoron et al., 2005) remained fairly constant throughout at least the past 1.75 million years, leading to a pronounced zonal SST contrast within the tropical oceans. Consequently, SSTs in the upwelling areas of the tropical oceans are thought to be controlled by the temperature of deeper waters formed at higher lati-

tudes, and therefore tend to reflect processes acting in the extra-tropics. The resulting cooling of the surface temperature leads to an enhanced land-ocean thermal gradient and hence may form a positive feedback.

As a result, two mechanisms are proposed to have caused the MPT and intensification of Northern Hemisphere ice sheet growth: the first invokes a gradual global cooling during the Pleistocene, possibly induced by decreasing atmospheric  $\text{CO}_2$ , until a threshold was passed after which feedbacks exerted by continental and/or marine ice-sheet dynamics became so dominant that they governed global temperature (Berger et al., 1999; Imbrie et al., 1993; Tziperman and Gildor, 2003). However, this hypothesis is strongly challenged by the stable SSTs in the WPWP (de Garidel-Thoron et al., 2005) and the early Pleistocene increase in benthic Mg/Ca (Billups and Schrag, 2002). Moreover, recent

atmospheric pCO<sub>2</sub> reconstructions do not show a long-term drawdown of the greenhouse gas during the early Quaternary (Hönisch et al., 2009).

The second mechanism suggests an important role for the tropics; the increased east–west temperature gradients, especially the one between the cold upwelling waters in the eastern Pacific and the thermally stable WPWP, invoked an increased Walker circulation. These changes might have led to atmospheric processes and oceanic interactions, which could have altered the meridional heat and moisture transfer to the Northern Hemisphere ice sheets during the MPT and thus contributed to the intensification of Northern Hemisphere glaciation (Philander and Fedorov, 2003; de Garidel-Thoron et al., 2005).

In contrast to the decoupling of tropical SSTs from the high latitudes and upwelling regions over the course of the Pleistocene, they co-vary on orbital timescales; SSTs in the tropical as well as the high-latitude oceans seem to have responded in phase with obliquity forcing (Liu and Herbert, 2004; de Garidel-Thoron et al., 2005; Medina-Elizalde and Lea, 2005) prior to the MPT. During obliquity maxima, global ice volume was reduced, and the global ocean warmed up. The fact that the tropical oceans show warming in pace with obliquity forcing implies that tropical SST changes are somehow related to high latitudes, since the amplitude of obliquity forcing at low latitudes is relatively small (de Garidel-Thoron, 2007). Another argument for assuming a strong coupling between high latitude forcing and low latitude SSTs is the absence of a dominant precessional signal in tropical SST records, although the local mean solar forcing in the tropical regions is dominated by precession. Therefore, it was hypothesised that meridional insolation gradients – driven by obliquity – are responsible for the tropical–extratropical coupling of climate signals rather than direct insolation (Raymo and Nisancioglu, 2003).

### 3.3.4 Late Quaternary (the ‘100-kyr world’)

As a consequence of internal feedbacks (involving CO<sub>2</sub>, dust, ice albedo and ice dynamics) rather than of external forcing, the large ice sheets that occurred

during the late Quaternary could grow gradually and be destroyed rapidly in the observed 100 000-year rhythm (Ruddiman, 2006), leading to the characteristic saw-tooth pattern of the late Pleistocene (Imbrie et al., 1993). The late Quaternary has known about ten glacial–interglacial cycles with slightly varying amplitudes and no clear long-term global temperature trend. Records from the equatorial Pacific indicate neither a long-term cooling, nor a general warming trend for the late Quaternary (Fig. 3.5). So far, there are no comparable SST records from the tropical Atlantic that continuously cover the last 1 Ma. One record covers the last 560 kyr (Martinez et al., 2007) of which the last 480 kyr are shown here (Fig. 3.6). The oldest 80 kyr are left out due to altered hydrographic conditions in this period (Martinez et al., 2007). Even these last 480 kyr show no clear temperature trend.

During the late Quaternary, the variability in tropical SST between glacial and interglacial times was smaller than the variability observed at high latitudes (e.g. CLIMAP Project Members, 1981; Pflaumann et al., 2003). From these high-latitude regions, the North Atlantic appeared to be the one area with the largest amplitudes in variability. The state of the tropical oceans during the Last Glacial Maximum (LGM) will be discussed in detail in the following section.

## 3.4 The past 20000 years

### 3.4.1 The Last Glacial Maximum

The first quantitative global reconstruction of SST during the LGM was produced by the ‘Climate Long-Range Investigation, Mapping and Prediction’ (CLIMAP, see also Chapter 9, section 9.3.2) project in the 1970s and 1980s (CLIMAP Project Members, 1981). CLIMAP’s statistically based SST reconstructions from planktonic microfossils resulted in estimates of global cooling of only 3.0 °C relative to modern day (Hoffert and Covey, 1992), with little to no change in the tropics. These results focused attention away from the tropics to extratropical regions, especially to the North Atlantic where glacial SST anomalies appeared to be most

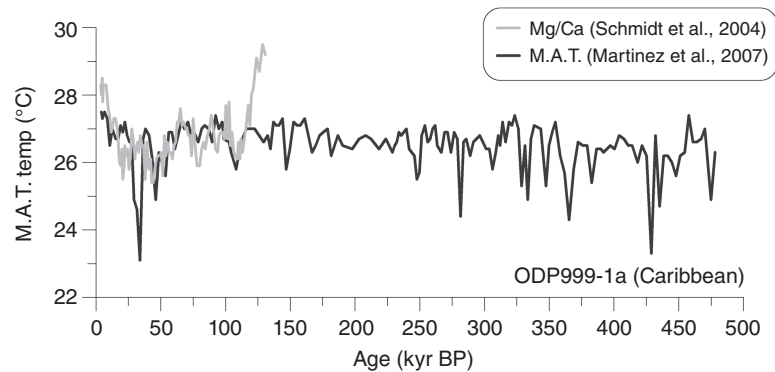


**Fig. 3.6** Quaternary SST records from the Caribbean. In light grey the Mg/Ca reconstruction by Schmidt et al. (2004) covering the last 140 ka BP. In dark grey the Modern-Analogue Technique (M.A.T.) reconstruction by Martinez et al. (2007) for the last 480 ka. The originally published record is 80 kyr longer but prior to 480 kyr BP the hydrographical conditions in the basin were completely different (Martinez et al., 2007). Data are from the PANGAEA database: [www.pangaea.de](http://www.pangaea.de).

substantial. A discrepancy between continental proxy records of tropical temperatures and CLIMAP tropical SST reconstructions, however, challenged the notion of a ‘tropical thermostat’. Moreover, atmospheric general circulation models forced with CLIMAP SST had problems in simulating glacial tropical climate as inferred from terrestrial proxy records (Pinot et al., 1999). By contrast, adding a tropical cooling to the CLIMAP reconstruction resulted in climate simulations that were in much better agreement with terrestrial archives (e.g. Lohmann and Lorenz, 2000) and showed substantial modifications of the tropical hydrologic cycle (Romanova et al., 2004). Taken together, it appeared that CLIMAP systematically overestimated the temperatures in the tropical oceans during the last glacial. More than one decade later, geochemical analyses of Barbados corals suggested a tropical SST that was 5°C colder (albeit with a large error bar) than present values 19 kyr ago (Guilderson et al., 1994), showing that there was an urgent need to re-evaluate the CLIMAP database.

Recently, a new global SST reconstruction for the LGM (19–23 kyr ago) was published by the ‘Multi-proxy Approach for the Reconstruction of the Glacial Ocean Surface’ (MARGO) project (MARGO Project Members, 2009). The MARGO compilation

combines almost 700 individual SST reconstructions based on all prevalent microfossil-based and geochemical palaeothermometers. In contrast to CLIMAP, tropical SST cooling is substantial in the MARGO reconstruction (Fig. 3.7a). Pronounced east–west gradients within each basin mark the equatorial oceans, with the strongest tropical anomalies in the Atlantic. Another remarkable feature of the tropical reconstructions is a 1–3°C cooling of the Western Pacific Warm Pool. State-of-the-art coupled climate models are not capable of simulating these glacial anomalies in the tropical oceans (as an example, an LGM simulation with the Community Climate System Model CCSM3 is shown in Fig. 3.7b). One possible error source in the currently available LGM simulations is the lack of a proper radiative forcing due to changes in the atmospheric aerosol load. In particular an enhanced concentration of mineral dust during generally drier glacial times is neglected in most simulations. Moreover, coastal upwelling is currently not properly resolved in global climate models owing to the use of relatively coarse grid resolutions.

### 3.4.2 Glacial termination: an active role for the tropics?

Based on the observational finding that tropical SST changes led the decrease of high-latitude

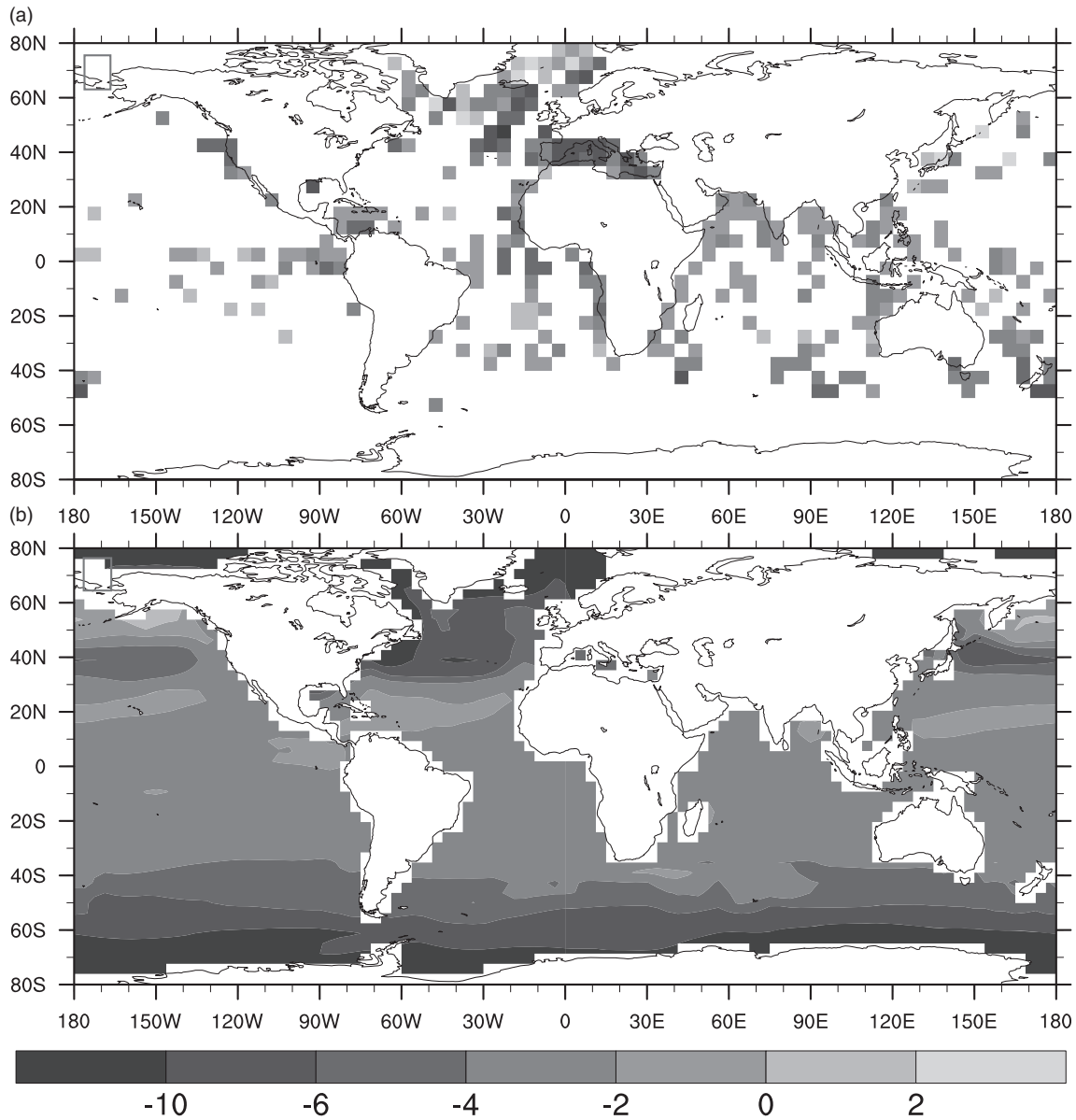


**Fig. 3.7** Average annual SST anomaly between Last Glacial Maximum and modern conditions based on the MARGO dataset (a) and on results from a comprehensive coupled climate model simulation using CCSM3 (b). MARGO data are available from <http://www.glacialoceanatlas.org>. Model simulations are described in Merkel et al. (2010).

Northern Hemispheric ice volume by 2–4 kyr, it has been suggested that the tropical oceans (in particular the Pacific) played an active role in triggering glacial terminations (Lea et al., 2000; Visser et al., 2003), although recently it was stated that the

Australian–Indonesian monsoon is coupled to the Northern Hemisphere (Mohtadi et al., 2011). Using an atmospheric general circulation model, Rodgers et al. (2003) showed that a moderate warming of tropical SSTs from glacial boundary conditions may

indeed cause a strong increase in summer temperatures over the Laurentide ice sheet.

The notion of a tropical glacial–interglacial trigger begs the question of which mechanism caused the tropical warming. The direct tropical response to orbital-induced insolation changes was suggested as a possible candidate. Using a coupled model of intermediate complexity for the equatorial Pacific (see Chapter 1, section 1.3; Chapter 9, section 9.4.1), Clement et al. (1999) showed that the precessional cycle with a periodicity of about 19–23 kyr has an influence on the period and amplitude of ENSO and, via non-linear rectification processes, also on the tropical mean state. However, the simulated mean state changes do not agree with temperature reconstructions from the eastern equatorial Pacific (Lea et al., 2000) both in terms of phase and amplitude, indicating that greenhouse gases (and, to a lesser degree, ice sheets) played a major role in determining tropical temperatures throughout the late Quaternary. Therefore, a more likely mechanism to cause tropical SST warming involves changes in the global carbon cycle. For such a mechanism, the Southern Ocean would probably play a crucial role since it is only in high latitudes that the atmosphere can interact with the deep ocean carbon reservoir. This hypothesis is corroborated by recent results of Stott et al. (2007) who determined the chronology of high- and low-latitude climate change at the last glacial termination by geochemical analysis of benthic and planktonic foraminifers from a sediment core recovered from the western tropical Pacific. They found that deep-sea temperatures increased by around 2 °C between 19 and 17 kyr BP, leading the deglacial rise in atmospheric CO<sub>2</sub> and tropical SST by about 1000 years. Both deep-sea warming and atmospheric CO<sub>2</sub> increase originated in the Southern Ocean, where deep-water masses are formed. Stott et al. (2007) suggested that the trigger for the initial deglacial warming of the Southern Ocean was an increase in local insolation during austral spring. The resulting retreat of sea ice would also promote enhanced ventilation of the deep sea and the subsequent rise in atmospheric CO<sub>2</sub>.

Whether the tropical oceans played a crucial role in forcing the demise of Northern Hemisphere ice

sheets remains an open question. Two modelling studies strongly challenge this notion. Rodgers et al. (2004) employed a thermomechanical ice sheet model, driven by the output of atmospheric general circulation models, to study the sensitivity of the Laurentide and Fennoscandian ice sheets to tropical SST changes during deglaciation. They found that the ice-sheet mass balance is not strongly sensitive to tropical SST boundary conditions, since the responses in surface temperature and precipitation over the ice sheets nearly compensate. The role of orbital-induced ENSO-type forcing of the Laurentide ice sheet retreat (Clement et al., 1999; Clement and Peterson, 2008) was recently questioned by Merkel et al. (2010). Using a comprehensive coupled climate model, they demonstrated that glacial boundary conditions induce major modifications to ENSO teleconnections and that the ‘blueprint’ of modern ENSO teleconnections should only be applied with caution to glacial climate periods. Finally, it is important to realise that alkenone-derived SST reconstructions do not show the same lead-lag relationship between the tropics and the high northern latitudes during the last terminations as Mg/Ca temperatures (see section 3.4.3).

Another role for the tropical oceans in shaping the last deglaciation was proposed by Schmidt et al. (2004). Based on hydrographic reconstructions from Caribbean Sea sediment cores, they suggested that the tropical Atlantic may act as a salt reservoir which regulates the delivery of high-salinity waters to the North Atlantic convection sites, thus affecting the Atlantic thermohaline circulation and the associated northward heat transport during terminations. A slowdown of the thermohaline circulation during cold stadials (e.g. Heinrich Event 1) would have led to an accumulation of salty waters in the tropical Atlantic. At the initiation of the warm Bølling/Allerød interval (14.6 kyr BP), tropical SSS dropped abruptly, suggesting that the export of salty tropical waters to the North Atlantic amplified the thermohaline overturning and contributed to northern high-latitude warming. Similar conclusions were derived by Weldeab et al. (2006) who analysed a sediment core from the continental margin of northeastern Brazil. They suggested that

the sudden release of accumulated salt in the western tropical Atlantic at the end of the Younger Dryas and Heinrich Event 1 contributed to the rapid reinvigoration of the Atlantic overturning circulation.

Despite these exciting results, it would be daring to claim that the deglacial history of the tropical Atlantic Ocean is well understood. For instance, there are inconsistent findings about SST changes in the southern Caribbean and in the western tropical Atlantic during the Younger Dryas when the

North (South) Atlantic generally cooled (warmed) in response to a weakening of the Atlantic thermohaline circulation. Figure 3.8 summarises reconstructed SST changes for the Younger Dryas stadial (Wan et al., 2009).

While data from Guilderson et al. (2001) and Lea et al. (2003) suggest a substantial cooling of the tropical west Atlantic, Rühlemann et al. (1999), Hüls and Zahn (2000) and Schmidt et al. (2004) found the opposite response. Whether this discrepancy is an artifact in the proxies (due to uncertain-

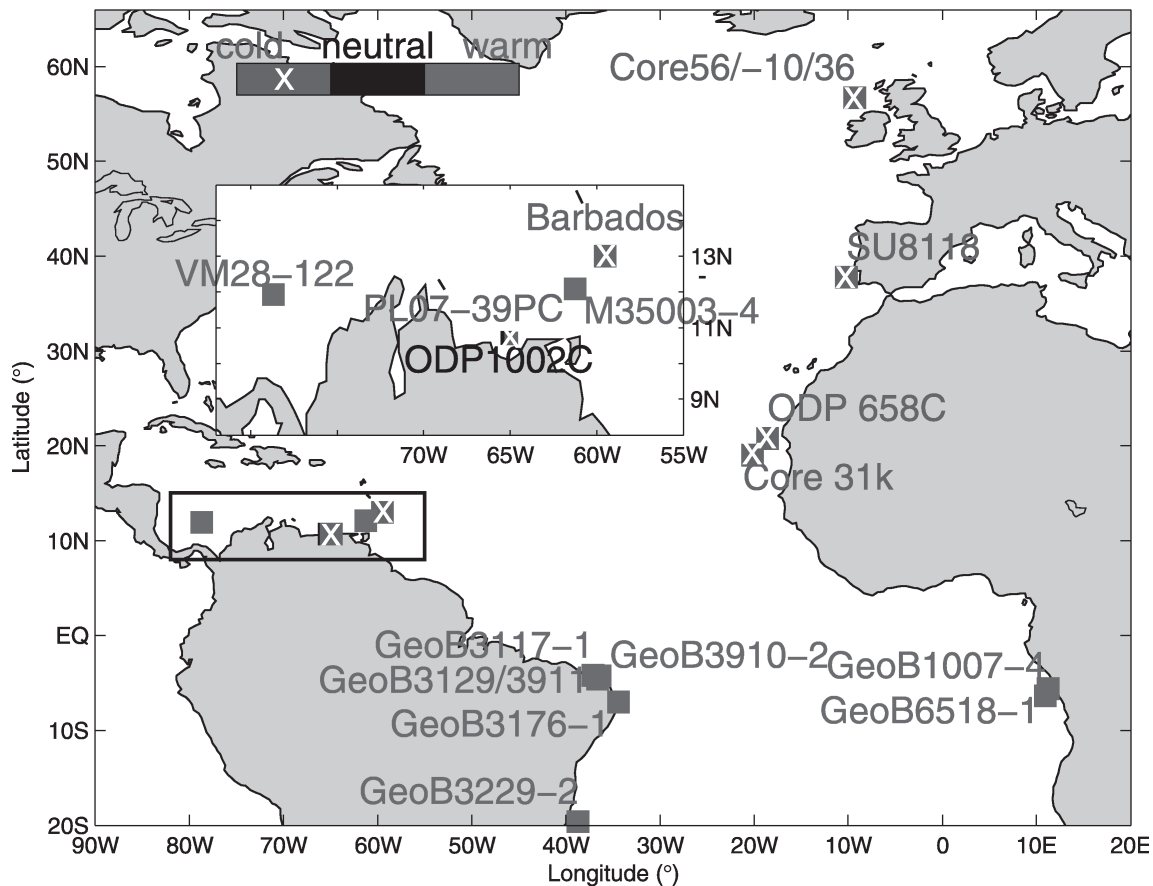


**Fig. 3.8** Atlantic SST response to a slowdown of the thermohaline circulation during the Younger Dryas stadial. Temperature anomalies suggested by proxy records are marked by squares (crossed squares indicate cooling) along with the names of the cores. The inset is an enlargement for the Caribbean and western tropical Atlantic. For references concerning the proxy data the reader is referred to Wan et al. (2009). Note the interhemispheric 'seesaw pattern' with cooling in the Northern Hemisphere and warming in the Southern Hemisphere. In the western tropical Atlantic, the picture is less clear. From Wan et al. (2009). Copyright (2009) American Geophysical Union. Reproduced with permission.

ties associated with seasonality, depth habitats, diagenesis, etc.) or a real feature is an open question. Based on ocean–atmosphere model experiments, Wan et al. (2009) suggested that the SST response to overturning slowdown over the Caribbean and western tropical Atlantic is complex and can vary considerably on small spatial scales. It is interesting to note that the subsurface temperature change in the tropical Atlantic was probably stronger than the surface response during the Younger Dryas and Heinrich Event 1, showing a rapid and intense warming (Rühlemann et al., 2004). For an overview of the even more complex and less understood deglacial SST history of the Indian Ocean (in particular the Arabian Sea), the reader is referred to Saher et al. (2007). The tropical Pacific will be discussed in detail in the following section.

### 3.4.3 History of the equatorial Pacific and the state of ENSO

Despite growing efforts to understand the climatic history of the equatorial Pacific, there is still no consensus about the ENSO state of this region during glacial episodes, or even the Holocene. A number of palaeoceanographic studies considered the ice age climate in the tropical Pacific as similar to a moderate ‘El Niño-like’ state (Koutavas et al., 2002; Stott et al., 2002; Koutavas and Lynch-Stieglitz, 2003), whereas other studies inferred that glacial Pacific climate resembled the cold phase of ENSO (Lea et al., 2000; Andreassen et al., 2001; Beaufort et al., 2001). Still other studies called on ice age linkages to higher latitudes that may reflect neither of the two ENSO states (Pisias and Mix, 1997; Feldberg and Mix, 2003).

Even more uncertainty arises regarding the last deglacial transition. Eastern tropical Pacific temperature records based on foraminiferal Mg/Ca suggest that warming in this region began as early as approximately 19–18kyr ago, preceding the major deglacial transition by several thousand years as discussed in the previous section (Lea et al., 2000, 2006; Koutavas et al., 2002; Benway et al., 2006). A similar early warming without interruptions is also observed in the upwelling regions off Peru (Feldberg and Mix, 2002). This

covariation between tropical Pacific SSTs and Antarctic and Southern Ocean temperatures implies a fundamental connection between the two regions. By contrast, many alkenone-derived tropical eastern Pacific SST records north and south of the equator (Kienast et al., 2006; Prahl et al., 2006; Pahnke et al., 2007; Koutavas and Sachs, 2008) show a cooling trend during the early deglaciation and a Northern Hemisphere timing of deglacial warming with significant SST reversals over the course of the termination, which probably corresponds to Heinrich Event 1 and the Younger Dryas (Kienast et al., 2006). This conflict can hardly be resolved by invoking different seasonal or interannual biases, ecological biases or time-varying dissolution effects (Mix, 2006). The controversy may rather indicate that, although the Antarctic warming signal may have been transferred into the equatorial Pacific, it was shaped by oceanic or atmospheric climate linkages between the tropical eastern Pacific and high northern latitudes. Possible candidates are, for example, changes in the Atlantic overturning circulation, shifts in the ITCZ position, Atlantic–Pacific atmospheric moisture transfer, and/or shifts in the ‘mean state’ of ENSO. The fact that a similar cooling during Heinrich Event 1 and the Younger Dryas was also observed in the South China Sea and the Sulu Sea in the western tropical Pacific (Huang et al., 2002; Rosenthal et al., 2003) also suggests a link to the east Asian monsoon system, possibly through large-scale changes in the ITCZ position and tropical Pacific ocean–atmosphere circulation (Kienast et al., 2006).

The nature of the connection between North Atlantic and tropical Pacific climate as well as its role in long-term and abrupt climate change remains elusive. A large number of proxy records indicate that millennial-scale North Atlantic cold events (e.g. Heinrich Event 1 and the Younger Dryas) were accompanied by a generally more southern position of the Atlantic ITCZ and of the tropical rainbelt over South America (Arz et al., 1998; Peterson et al., 2000; Haug et al., 2001). It has recently been suggested that this may also hold true for the eastern tropical Pacific (Benway et al., 2006; Kienast et al., 2006; Leduc et al., 2007). Some studies even suggested a more ‘El Niño-like’

state of the Pacific during stadials (McIntyre and Molfino, 1996; Stott et al., 2002; Turney et al., 2004), possibly favoured by feedbacks in the thermohaline circulation (Timmermann et al., 2005). A recent study, however, questioned the hypothesis of a warm ENSO phase in the Pacific during Heinrich Event 1 and the Younger Dryas (Koutavas and Sachs, 2008). The authors point out that low alkenone-derived SSTs in the cold tongue area as well as high productivity near Galapagos (e.g. Kienast et al., 2006; Koutavas and Sachs, 2008) are inconsistent with a southern position of the Pacific ITCZ and/or with a permanent 'El Niño-like' state during stadials. This argues for contrasting ITCZ movements in the Atlantic and Pacific at the terminations of North Atlantic cold events, as observed today associated with ENSO (Enfield and Mayer, 1997; Prange et al., 2010). If such an ENSO-like adjustment is indeed part of the Atlantic–Pacific communication mechanism, however, it would imply El Niño-like shifts during interstadials (Koutavas and Sachs, 2008), rather than during stadials (Stott et al., 2002).

The major drawback of most proxy records, however, consists in their lack of sufficient temporal resolution to explicitly resolve ENSO in its original definition of an interannual climate variability phenomenon. These records allow statements to be made about mean state changes (Koutavas et al., 2002; Pena et al., 2008) but only indirectly about variability changes, with mean state changes also bearing the potential of being induced by changes in the skewness of SST probability density functions. In this respect, fossil corals provide a unique opportunity to reconstruct past tropical SST fluctuations on a year-to-year basis and even subannually (e.g. Asami et al., 2009). Another way of studying ENSO variability in the past is by numerical approaches using climate models of different complexities, with some models being restricted to the tropical Pacific (Clement et al., 1999) and some models representing the global fully coupled atmosphere–ocean system (e.g. Otto-Bliesner et al., 2003; Peltier and Solheim, 2004) (see also Chapter 9, section 9.4). In the latter category, the first comprehensive modelling approach for studying ENSO variability in past glacial climates beyond LGM

climate has been presented in a recent study focusing on the LGM, Heinrich Stadial 1 as well as MIS3 stadial and interstadial simulations (Merkel et al., 2010). Interestingly, the Heinrich Stadial 1 simulation exhibits the most pronounced response of eastern tropical Pacific interannual variability showing a marked intensification in response to the combination of glacial boundary conditions and freshwater hosing in the North Atlantic. With glacial boundary conditions alone, only minor changes of ENSO are found for both LGM and MIS3 stadial and interstadial climatic states. A central role is therefore hypothesised for a slowdown of the Atlantic meridional overturning circulation and a subsequent modification – via atmospheric teleconnections to the eastern tropical Pacific – of the meridional SST gradient, the annual cycle of SST and SST interannual variability (Timmermann et al., 2007; Merkel et al., 2010). These model results lead to conclusions that are clearly different from those of the study by Leduc et al. (2009) analysing time windows of the last glacial period. Based on planktonic foraminifera representing the eastern tropical Pacific thermocline, the largest variability is reported at the beginning of Marine Isotope Stage 3 (around Dansgaard–Oeschger interstadial 14), with only weak differences between different time windows (Holocene, Heinrich Stadial 1, LGM, Dansgaard–Oeschger interstadial 8, Heinrich Stadial 4). Most strikingly, the simulated remarkable ENSO response during Heinrich Stadial 1 (Merkel et al., 2010) is not reflected at all in the reconstructions of  $\delta^{18}\text{O}$  at thermocline depths.

Therefore, there is a clear need for future research to disentangle the interactions between tropical Pacific mean state and variability (Rosenthal and Broccoli, 2004), even for modern climate conditions, in order to shed more light on the interpretation of proxy records that do not explicitly resolve interannual ENSO variability, with the ultimate goal to reconcile palaeodata with model results for past climatic states.

#### 3.4.4 The Holocene

There is growing evidence for pronounced changes in the amplitude and frequency of ENSO over the

course of the Holocene. For example, palaeoclimate records from a small lake in the high Andes of Ecuador (Rodbell et al., 1999; Moy et al., 2002) (see Chapter 8, section 8.4) and from a lake on the Galapagos Islands (Riedinger et al., 2002) indicate that ENSO variability did not become active until about 6–5 kyr BP. Coral records from the western Pacific (Tudhope et al., 2001) show that ENSO variability was present during the middle Holocene (~6.5 kyr BP), albeit with reduced amplitudes. It is still not clear how long-term changes in the ‘mean ENSO’ state of the tropical Pacific, possibly connected to orbitally driven changes in insolation (e.g. Clement et al., 1999), accompanied the marked changes in ENSO variability over the course the Holocene. In particular, a continuing middle Holocene controversy is whether the mean state of the tropical Pacific was warmer or colder than today (Cane, 2005).

A large number of palaeoclimate studies from different parts of the globe indicate that El Niño was suppressed during the middle Holocene (McGlone et al., 1992; Shulmeister and Lees, 1995; Haberle et al., 2001; Haberle and Ledru, 2001; Gagan et al., 2004; Hong et al., 2005; Brijker et al., 2007). Based on SST reconstructions in the eastern Pacific cold tongue region and in the WPWP (Koutavas et al., 2002, 2006; Stott et al., 2004), it has been suggested that the tropical Pacific was more ‘El Niño-like’ during the early and late Holocene, and in a more ‘La Niña-like’ mean state during the middle Holocene (~8–5 kyr BP). The observed increase in cold tongue SSTs after 5 kyr (Koutavas et al., 2002) would be in line with a southward movement of the ITCZ. Rein et al. (2005) also showed a suppression of El Niño during the middle Holocene (c. 8–5 kyr BP) and increased ENSO variability during the early and late Holocene in a high-resolution marine sediment record off the coast of Peru. A period of weak El Niño activity during the mid Holocene is further documented in geological (Colinvaux, 1972; Keefer et al., 1998) and archaeological (Núñez et al., 2002) data from the Galapagos Islands and South America. On the basis of warm water mollusc shells found at the coast of Peru, however, Sandweiss et al. (1996, 2001; see also Chapter 8, section 8.7.1) inferred

that mean water temperatures were higher prior to 5.8 kyr BP – indicative of a persistent El Niño-like state (see also Andrus et al., 2002). The successive cooling after 5.8 kyr BP has been ascribed to increased upwelling of cool water between El Niño events. This is corroborated by high  $^{14}\text{C}$  reservoir ages found in mollusc shells on the Peru margin after around 4 kyr BP (Fontugne et al., 2004). Low-resolution foraminiferal stable isotope records from the eastern Pacific cold tongue region point to enhanced upwelling of cool, nutrient-rich subsurface waters since 7 kyr BP (Loubere et al., 2003). Superimposed on these (still controversially discussed) long-term changes, ENSO variability may also have operated on millennial timescales throughout the Holocene (e.g. Moy et al., 2002; Hong et al., 2005). Rodbell et al. (1999) and Moy et al. (2002) found alternating periods of high and low ENSO variability in lake sediments of Ecuador, whereas periods of low ENSO variability tended to occur during periods of ice rafting in the North Atlantic (so-called ‘Bond Events’). Hong et al. (2005) came to a similar conclusion by studying changes in the monsoon system.

Long- and short-term variations in ENSO, in the position of the ITCZ and in the wind field over the eastern tropical Pacific would have altered the atmospheric freshwater export from the tropical Atlantic over the course of the Holocene (Stott et al., 2004; Pahnke et al., 2007) with potential effects on the global conveyor belt circulation. Stott et al. (2004) argue that high SSS in the western tropical Pacific during the early Holocene climate optimum may have been caused by northward displacement of the ITCZ over Central America (Haug et al., 2001), which would act to trap water vapour within the Atlantic and reduce the atmospheric moisture transport across the Central American isthmus. Freshening of the sea surface in the Western Pacific Warm Pool over the course of the Holocene would be in line with increasing water vapour transfer from the Atlantic into the Pacific due to a gradual southward shift of the ITCZ in response to changing precessional forcing of solar radiation (Stott et al., 2004).

Numerical models may provide further insight into the tropical climate history of the Holocene

(see Chapter 9, sections 9.2 and 9.4.1). Important findings on mid Holocene ENSO behaviour have been achieved by using the Zebiak–Cane anomaly model of the tropical Pacific only (Clement et al., 1999). First steps towards a comprehensive representation of tropical ocean mean state and variability have been made in the framework of the second phase of the Paleoclimate Modelling Intercomparison Project (PMIP2). In contrast to the first phase of PMIP, fully coupled global ocean–atmosphere models have become available to test the climate response to mid Holocene boundary conditions (6 kyr BP). An intercomparison of tropical Pacific changes of mean state and variability within the different models has been presented by Zheng et al. (2008). Most of the PMIP2 models simulate a significant cooling over large parts of the tropical Pacific as well as a decrease in the amplitude of ENSO variability. This is attributed to the enhancement of tropical easterlies and a strengthening of upwelling thereby suppressing El Niño events. Additionally, although the Northern Hemisphere seasonal cycle is enhanced at 6 kyr BP, the seasonal cycle over the eastern tropical Pacific is dampened at 6 kyr BP which emphasises the role of feedbacks in the climate system. However, it also has to be taken into account that the tropical Pacific is subject to extra-tropical influences which are communicated into the tropical Pacific region via teleconnections from the whole Pacific realm (see Schneider, et al., 1999; Matei et al., 2008; Chiang et al., 2009).

Thanks to increasing computer processing power, transient simulations using comprehensive coupled climate models are now becoming available. Upon analysing transient ensemble climate simulations with a coupled atmosphere–ocean model under accelerated orbitally driven insolation forcing for the last 7000 years, Lorenz et al. (2006) described a global heterogenic spatial trend pattern for SST, in which the extra-tropics cooled while the tropics experienced a warming. The authors attributed these divergent Holocene climate trends to seasonally opposing insolation changes. These SST changes are consistent with mid Holocene time slice experiments. By contrast, the simulated temperature trend in the thermocline is dominated by an anti-

symmetric pattern with a long-term warming (cooling) in the northern (southern) hemisphere mid latitudes, and a cooling in most parts of the tropics (Liu et al., 2003).

### 3.5 Outlook

Proxy records and observations from the instrumental period can provide a window into the past, thereby underlining the relevance of tropical climate and its variability. Such records can also provide the long-term context through which natural and anthropogenic climate change can be evaluated. Future perspectives, however, can only be, and have already been, widely addressed within a climate modelling framework, which, among other foci, allows us to tackle the highly relevant role of the tropics for global climate. It is of utmost importance to study whether the sensitive and detailed multi-faceted interactions within the tropics and dynamical couplings between the tropics and extra-tropics will be maintained in the future.

A majority of simulations suggests a large-scale although not spatially uniform warming of the tropical oceans. From their twenty-first century simulation with a complex coupled atmosphere–ocean model, which adequately resolves tropical Pacific dynamics, Timmerman et al. (1999) concluded that the tropical Pacific climate will change towards a mean state resembling present-day El Niño conditions. Furthermore, their results point to more frequent El Niño events as well as stronger La Niña events superimposed on mean-state changes. In a recent multimodel intercomparison of future climate scenario simulations, however, the dependency of tropical ocean responses on the respective model performance and the result of rather weak-amplitude changes are emphasised (Collins and the CMIP modelling groups, 2005). These models still exhibit interannual variability superimposed on the change in the mean state. For the models used in the IPCC Fourth Assessment Report, Van Oldenborgh et al. (2005) advise caution when specifying the degree of uncertainty about the relative strength of ENSO events in a green-

house world. Consequently, in the IPCC AR4 (IPCC, 2007), it is concluded that for ENSO, there is '... no consistent picture of how it might be expected to change in response to anthropogenic forcing' (see also Chapter 11, Section 11.3.1).

Although tropical Pacific climate is an important driver of tropical atmosphere–ocean variations, climate interactions taking place in the Atlantic and Indian Ocean basins also need to be taken into account. How the ITCZ, monsoon activity, the Indian Ocean Dipole and their respective signatures within the ocean will be modulated by anthropogenic climate change, has to be addressed in most comprehensive approaches involving hierarchies of spatial and temporal scales for which palaeoceanographic data may provide important long term-based references.

For a future perspective, there is also a clear need for closer insights into land–ocean interactions such as changes in land-use which impact on the mineral dust input into the atmosphere and, via modulations of the radiative balance, on sea surface temperature (e.g. Evan et al., 2009). Through its fertilising effect, mineral dust may also influence ocean productivity and carbon uptake by the ocean biosphere (Jickells et al., 2005), which strongly advocates for integrated approaches of climate–biogeochemistry analysis. However, we are optimistic that our understanding of the tropical ocean's future and tropical dynamics can be improved by further looking at the past and by utilising the synergy that evolves from a closer liaison between climate modellers, observationalists and palaeoceanographers.

## References

- Alexander, M.A., Bladé, I., Newman, M., et al. (2002) The atmospheric bridge: the influence of ENSO teleconnections on air–sea interaction over the global oceans. *Journal of Climate* **15**, 2205–2231.
- Anand, P., Elderfield, H. and Conte, M.H. (2003) Calibration of Mg/Ca thermometry in planktonic foraminifera from sediment trap time series. *Paleoceanography* **18**, PA000846.
- Andreasen, D.H., Ravelo, A.C. and Broccoli, A.J. (2001) Remote forcing at the Last Glacial Maximum in the tropical Pacific Ocean. *Journal of Geophysical Research* **106**, 879–897.
- Andrus, C.F.T., Crowe, D.E. and Romanek, C.S. (2002) Oxygen isotope record of the 1997–1998 El Niño in Peruvian sea catfish (*Galeichthys pervianus*) otoliths. *Paleoceanography* **17**, 1053. doi:10.1029/2001PA000652.
- Antonov, J.I., Locarnini, R.A., Boyer, T.P., et al. (2006) *World Ocean Atlas 2005*, Volume 2: Salinity. Levitus, S., (Ed.) NOAA Atlas NESDIS 62, U.S. Government Printing Office, Washington D.C., pp. 182.
- Arz, H.W., Patzold, J. and Wefer, G. (1998) Correlated millennial-scale changes in surface hydrography and terrigenous sediment yield inferred from last-glacial marine deposits off northeastern Brazil. *Quaternary Research* **50**, 157–166.
- Asami, R., Felis, T., Deschamps, P., et al. (2009) Evidence for tropical South Pacific climate change during the Younger Dryas and the Bølling/Allerød from geochemical records of fossil Tahiti corals. *Earth and Planetary Science Letters* **288**, 96–107.
- Ashok, K., Guan, Z. and Yamagata, T. (2001) Impact of the Indian Ocean Dipole on the relationship between the Indian monsoon rainfall and ENSO. *Geophysical Research Letters* **28**, 4499–4502.
- Beaufort, L., de Garidel-Thoron, T., Mix, A.C. and Pisias, N.G. (2001) ENSO-like forcing on oceanic primary production during the Late Pleistocene. *Science* **293**, 2440–2444.
- Beck, J.W., Edwards, R.L., Ito, E., et al. (1992) Sea-surface temperature from coral skeletal strontium/calcium ratios. *Science* **257**, 644–647.
- Bemis, B.E., Spero, H.J., Bijma, J. and Lea, D.W. (1998) Reevaluation of the oxygen isotopic composition of planktonic foraminifera: experimental results and revised paleotemperature equations. *Paleoceanography* **13**, 150–160.
- Benway, H.M., Mix, A.C., Haley, B.A. and Klinkhammer, G.P. (2006) Eastern Pacific Warm Pool paleosalinity and climate variability: 0–30 kyr. *Paleoceanography* **21**, PA3008, doi:10.1029/2005PA001208.
- Berger, A., Li, X.S. and Loutre, M.F. (1999) Modelling northern hemisphere ice volume over the last 3 Ma. *Quaternary Science Reviews* **18**, 1–11.
- Billups, K. and Schrag, D.P. (2002) Paleotemperatures and ice volume of the past 27 Myr revisited with paired Mg/Ca and <sup>18</sup>O/<sup>16</sup>O measurements on benthic foraminifera. *Paleoceanography* **17**, 1003, doi:10.1029/2000PA000567.
- Bjerknes, J. (1969) Atmospheric teleconnections from the equatorial Pacific. *Monthly Weather Review* **97**, 163–172.

- Bond, G., Heinrich, H., Broecker, W.S., et al. (1992) Evidence for massive discharges of icebergs into the North Atlantic ocean during the last glacial period. *Nature* **360**, 245–249.
- Braconnot, P., Otto-Bliesner, B., Harrison, S., et al. (2007a) Results of PMIP2 coupled simulations of the Mid-Holocene and last glacial maximum – Part 1: experiments and large-scale features. *Climate of the Past* **3**, 261–277.
- Braconnot, P., Otto-Bliesner, B., Harrison, S., et al. (2007b) Results of PMIP2 coupled simulations of the Mid-Holocene and Last Glacial Maximum – Part 2: feedbacks with emphasis on the location of the ITCZ and mid- and high latitudes heat budget. *Climate of the Past* **3**, 279–296.
- Braconnot, P., Marzin, C., Grégoire, L., et al. (2008) Monsoon response to changes in Earth's orbital parameters: comparisons between simulations of the Eemian and of the Holocene. *Climate of the Past* **4**, 281–294.
- Brassell, S.C., Eglinton, G., Marlowe, I.T., et al. (1986) Molecular stratigraphy: a new tool for climatic assessment. *Nature* **320**, 129–133.
- Brijker, J., Jung, S.J.A., Ganssen, G., et al. (2007) ENSO-related decadal scale climate variability from the Indo-Pacific Warm Pool. *Earth and Planetary Science Letters* **253**, 67–82.
- Broecker, W.S. (1989) The salinity contrast between the Atlantic and Pacific oceans during glacial time. *Paleoceanography* **4**, 207–212.
- Broecker, W.S. (1991) The great ocean conveyor. *Oceanography* **4**, 79–89.
- Broecker, W.S., Kennett, J.P., Flower, B., et al. (1989) The routing of Laurentide ice-sheet meltwater during the Younger Dryas event. *Nature* **341**, 318–321.
- Broecker, W.S., Peteet, D.M. and Rind, D. (1985) Does the ocean-atmosphere system have more than one stable mode of operation? *Nature* **315**, 21–26.
- Cane, M.A. (2005) The evolution of El Niño, past and future. *Earth and Planetary Science Letters* **230**, 227–240.
- Chang, P., Ji, L. and Li, H. (1997) A decadal climate variation in the tropical Atlantic Ocean from thermodynamic air-sea interactions. *Nature* **385**, 516–518.
- Chang, P., Fang, Y., Saravanan, R., Ji, L. and Seidel, H. (2006) The cause of the fragile relationship between the Pacific El Niño and the Atlantic Niño. *Nature* **443**, 324–328.
- Chiang, J.C.H., Fang, Y. and Chang, P. (2009) Pacific climate change and ENSO activity in the mid-Holocene. *Journal of Climate* **22**, 923–939.
- Christian, J.R. and Murtugudde, R. (2003) Tropical Atlantic variability in a coupled physical-biogeochemical ocean model. *Deep Sea Research II* **50**, 2947–2969.
- Clark, P.U., Archer, D., Pollard, D., et al. (2006) The middle Pleistocene transition: characteristics, mechanisms, and implications for long-term changes in atmospheric pCO<sub>2</sub>. *Quaternary Science Reviews* **25**, 3150–3184.
- Clement, A.C. and Cane, M.A. (1999) A role for the tropical Pacific coupled Ocean-Atmosphere System on Milankovitch and millennial timescales part I: modeling study of tropical Pacific variability. In: Clark, P.U., Webb, R.S., Keigwin, L.D. (eds), *Mechanisms of global climate change at millennial time scales*. American Geophysical Union, Washington, D.C., pp. 23–34.
- Clement, A.C. and Peterson, L.C. (2008) Mechanisms of abrupt climate change of the last glacial period. *Reviews of Geophysics* **46**, RG4002.
- Clement, A.C., Seager, R. and Cane, M.A. (1999) Orbital controls on the El Niño/Southern Oscillation and the tropical climate. *Paleoceanography* **14**, 441–456.
- Clement, A.C., Seager, R., Cane, M.A. and Zebiak, S.E. (1996) An ocean dynamical thermostat. *Journal of Climate* **9**, 2190–2196.
- CLIMAP Project Members (1981) *Seasonal reconstructions of the Earth's surface at the last glacial maximum*. GSA Map and Chart Ser. MC-36, Boulder, Colorado.
- Colinvaux, P.A. (1972) Climate and the Galapagos Islands. *Nature* **240**, 17–20.
- Collins, M., the CMIP modelling groups (2005) EL Niño or La Niña-like climate change? *Climate Dynamics* **24**, 89–104.
- Collins, J.A., Schefuß, E., Heslop, D., et al. (2011) Interhemispheric symmetry of the tropical African rainbelt over the past 23,000 years. *Nature Geoscience* **4**, 42–45.
- Corrège, T., Delcroix, T., Récy, J., et al. (2000) Evidence for stronger El Niño-Southern oscillation (ENSO) events in a mid-Holocene massive coral. *Paleoceanography* **15**, 465–470.
- Craig, H. (1961) Isotopic variations in meteoric waters. *Science* **133**, 1702–1703.
- Csanady, G.T., 1984. The influence of wind stress and river runoff on a shelf-sea front. *Journal of Physical Oceanography* **14**, 1383–1392.
- Darbyshire, M. (1966) The surface waters near the coasts of Southern Africa. *Deep Sea Research and Oceanographic Abstracts* **13**, 57–81.
- Davey, M.K., Huddleston, M., Sperber, K.R., et al. (2002) STOIC – a study of coupled model climatology and

- variability in tropical ocean regions. *Climate Dynamics* **18**, 403–420.
- de Garidel-Thoron, T. (2007) Paleooceanography, records. In: Elias, S. (ed.), *Encyclopedia of Quaternary Sciences*. Elsevier, Amsterdam, pp. 1785–1793.
- de Garidel-Thoron, T., Rosenthal, Y., Bassinot, F. and Beaufort, L. (2005) Stable sea surface temperatures in the western Pacific warm pool over the past 1.75 million years. *Nature* **433**, 294–298.
- Dekens, P.S., Lea, D.W., Pak, D.K. and Spero, H.J. (2002) Core top calibration of Mg/Ca in tropical foraminifera: refining paleotemperature estimation. *Geochemistry, Geophysics, Geosystems* **3**, GC00200.
- Elderfield, H. and Ganssen, G. (2000) Past temperature and  $\delta^{18}\text{O}$  of surface ocean waters inferred from foraminiferal Mg/Ca ratios. *Nature* **405**, 442–445.
- Emiliani, C. (1955) Pleistocene temperatures. *Journal of Geology* **63**, 538–578.
- Enfield, D.B. and Mayer, D.A. (1997) Tropical Atlantic sea surface temperature variability and its relation to El Niño-Southern Oscillation. *Journal of Geophysical Research* **102**, 929–945.
- Englebrecht, A.C. and Sachs, J.P. (2005) Determination of sediment provenance at drift sites using hydrogen isotopes and unsaturation ratios in alkenones. *Geochimica et Cosmochimica Acta* **69**, 4253–4265.
- Epstein, S., Buchsbaum, R., Lowenstam, H.A. and Urey, H.C. (1953) Revised carbonate-water isotopic temperature scale. *Geological Society of America Bulletin* **64**, 1315–1326.
- Erez, J. and Luz, B. (1983) Experimental paleotemperature equation for planktonic foraminifera. *Geochimica et Cosmochimica Acta* **47**, 1025–1031.
- Esper, J., Cook, E.R. and Schweingruber, F.H. (2002) Low-frequency signals in long tree-ring chronologies for reconstructing past temperature variability. *Science* **295**, 2250–2253.
- Evan, A. T., Vimont, D.J., Heidinger, A.K., et al. (2009) The role of aerosols in the evolution of tropical North Atlantic Ocean temperature anomalies. *Science*, **234**, 778–781.
- Eyles, N., Eyles, C.H. and Gostin, V.A. (1997) Iceberg rafting and scouring in the Early Permian Shoalhaven Group of New South Wales, Australia: evidence of Heinrich-like events? *Palaeogeography, Palaeoclimatology, Palaeoecology* **136**, 1–17.
- Fairbanks, R.G. (1989) A 17,000-year long glacio-eustatic sea level record: influence of glacial melting rates on the Younger Dryas event and deep-ocean circulation. *Nature* **342**, 637–642.
- Fairbanks, R.G., Charles, C.D. and Wright, J.D. (1992) Origin of global meltwater pulses. In: Taylor, R.E., Long, A., Kra, R.S. (eds), *Radiocarbon after Four Decades*. Springer-Verlag, Berlin Heidelberg New York, pp. 473–500.
- Feldberg, M.J. and Mix, A.C. (2002) Sea-surface temperature estimates in the Southeast Pacific based on planktonic foraminiferal species; modern calibration and Last Glacial Maximum. *Marine Micropaleontology* **44**, 1–29.
- Feldberg, M.J. and Mix, A.C. (2003) Planktonic foraminifera, sea surface temperatures, and mechanisms of oceanic change in the Peru and south equatorial currents, 0–150 ka BP. *Paleoceanography* **18**, 1016.
- Felis, T., and Pätzold, J. (2004) Corals as climate archive. In: Fischer, H., Kumke, T., Lohmann, G., et al. (eds) *The Climate in Historical Times*. Springer-Verlag, Berlin. 483 pp.
- Fontugne, M., Carré, M., Bentaleb, I., Julien, M. and Lavallée, D. (2004) Radiocarbon reservoir age variations in the south Peruvian upwelling during the Holocene. *Radiocarbon* **46**, 531–537.
- Frenz, M., Höppner, R., Stuut, J.-B.W., et al. (2003) Surface sediment bulk geochemistry and grain-size composition related to the oceanic circulation along the South American continental margin in the Southwest Atlantic. In: Wefer, G., Mulitza, S. and Ratmeyer, V. (eds) *The South Atlantic in the Late Quaternary – Reconstruction of Material Budgets and Current Systems*. Springer Verlag, Berlin, pp. 347–373.
- Gagan, M.K., Hendy, E.J., Haberle, S.G. and Hantoro, W.S. (2004) Post-glacial evolution of the Indo-Pacific Warm Pool and El Niño-Southern Oscillation. *Quaternary International* **118–119**, 127–143.
- Ganopolski, A. and Rahmstorf, S. (2001) Rapid changes of glacial climate simulated in a coupled climate model. *Nature* **409**, 153–158.
- Giannini, A., Saravanan, R., and Chang, P. (2003) Oceanic forcing of Sahel rainfall on interannual to interdecadal time scales. *Science* **302**, 1027–1030.
- Guilderson, T.P., Fairbanks, R.G. and Rubenstone, J.L. (1994) Tropical temperature variations since 20,000 years ago: modulating interhemispheric climate change. *Science* **263**, 663–665.
- Guilderson, T.P., Fairbanks, R.G. and Rubenstone, J.L. (2001) Tropical Atlantic coral oxygen isotopes: glacial-interglacial sea surface temperatures and climate change. *Marine Geology* **172**, 75–89.
- Guilyardi, E. (2006) El Niño-mean state-seasonal cycle interactions in a multi-model ensemble. *Climate Dynamics* **26**, 329–348.

- Haberle, S.G., Hope, G.S. and van der Kaars, S. (2001) Biomass burning in Indonesia and Papua New Guinea: natural and human induced fire events in the fossil record. *Palaeogeography, Palaeoclimatology, Palaeoecology* **171**, 259–268.
- Haberle, S.G. and Ledru, M.-P. (2001) Correlations among charcoal records of fires from the past 16,000 years in Indonesia, Papua New Guinea, and Central and South America. *Quaternary Research* **55**, 97–104.
- Haug, G.H., Hughen, K.A., Sigman, D.M., et al. (2001) Southward migration of the Intertropical Convergence Zone through the Holocene. *Science* **293**, 1304–1308.
- Hendy, E.J., Gagan, M.K., Alibert, A., et al. (2002) Abrupt decrease in tropical Pacific sea surface salinity at the end of the Little Ice Age. *Science* **295**, 1511–1514.
- Hoffert, M.I. and Covey, C. (1992) Deriving global climate sensitivity from paleoclimate reconstructions. *Nature* **360**, 573–576.
- Holz, C., Stuut, J.-B.W. and Henrich, R. (2004) Terrigenous sedimentation processes along the continental margin off NW-Africa: implications from grain-size analyses of surface sediments. *Sedimentology* **51**, 1145–1154.
- Holz, C., Stuut, J.-B.W., Henrich, R. and Meggers, H. (2007) Variability in terrigenous sedimentation processes off northwest Africa and its relation to climate changes: inferences from grain-size distributions of a Holocene marine sediment record. *Sedimentary Geology* **202**, 499–508.
- Hong, Y.T., Hong, B., Lin, Q.H., et al. (2005) Inverse phase oscillations between the East Asian and Indian Ocean summer monsoons during the last 12000 years and paleo-El Niño. *Earth and Planetary Science Letters* **231**, 337–346.
- Hönisch, B., Hemming, N.G., Archer, D., et al. (2009) Atmospheric carbon dioxide concentration across the Mid-Pleistocene Transition. *Science* **324**, 1551–1554.
- Huang, C.-C., Chen, M.-T., Lee, M.-Y., et al. (2002) Planktonic foraminifera sea surface temperature records of the past two glacial terminations in the South China Sea near Wan-An shallow (Images core MD97-2151). *Western Pacific Earth Sciences* **2**, 1–14.
- Huguet, C., Schimmelmann, A., Thunell, R., et al. (2007) A study of the TEX86 paleothermometer in the water column and sediments of the Santa Barbara Basin, California. *Paleoceanography* **22**, PA3203-1–PA3203-9.
- Hüls, M. and Zahn, R. (2000) Millennial-scale sea surface temperature variability in the western tropical North Atlantic from planktonic foraminiferal census counts. *Paleoceanography* **15**, 659–678.
- Imbrie, J. and Kipp, N.G. (1971) A new micropaleontological method for quantitative paleoclimatology: application to a late Pleistocene Caribbean core. In: Turekian, K. (ed.), *The Late Cenozoic Ice Ages*. Yale University Press, New Haven and London, pp. 71–181.
- Imbrie, J., Boyle, E.A., Clemens, S.C., et al. (1992) On the structure and origin of major glaciation cycles 1. Linear responses to Milankovitch forcing. *Paleoceanography* **7**, 701–738.
- Imbrie, J., Berger, A., Boyle, E.A., et al. (1993) On the structures and origin of major glaciation cycles 2. the 100,000-year cycle. *Paleoceanography* **8**, 699–735.
- IPCC (2007) Climate Change 2007: the physical science basis. In: Solomon, S., Qin, D., Manning, M., et al. (eds), *Contribution of Working Group I to the Fourth Assessment Report of the Intergovernmental Panel on Climate Change*. Cambridge University Press, Cambridge, p. 996.
- Jickells, T. D., An, Z. S., Andersen, K. K., et al. (2005), Global iron connections between desert dust, ocean biogeochemistry, and climate. *Science* **308**, 67–71.
- Jin, F.-F., Kug, J.-S., An, S.-I. and Kang, I.-S. (2003) A near-coupled ocean-atmosphere mode in the equatorial Pacific Ocean. *Geophysical Research Letters* **30**, 521–524.
- Keefer, D.K., de France, S.D., Moseley, M.E., et al. (1998) Early maritime economy and El Niño events at Quebrada Tacahuay, Peru. *Science* **281**, 1833–1835.
- Keenlyside, N., Latif, M. and Dürkop, A. (2007) On sub-ENSO Variability. *Journal of Climate* **20**, 3452–3469.
- Kienast, M., Kienast, S.S., Calvert, S.E., et al. (2006) Eastern Pacific cooling and Atlantic overturning circulation during the last deglaciation. *Nature* **443**, 846–849.
- Kim, S.T. and O'Neil, J.R. (1997) Equilibrium and nonequilibrium oxygen isotope effects in synthetic carbonates. *Geochimica et Cosmochimica Acta* **61**, 3461–3475.
- Knauss, J.A. and Taft, B.A. (1963) Measurements of currents along the equator in the Indian Ocean. *Nature* **198**, 376–377.
- Koutavas, A. and Lynch-Stieglitz, J. (2003) Glacial-interglacial dynamics of the eastern equatorial Pacific cold tongue – Intertropical Convergence Zone system reconstructed from oxygen isotope records. *Paleoceanography* **18**, 1089, doi:10.1029/2003PA000894.
- Koutavas, A., deMenocal, P.B., Olive, G.C. and Lynch-Stieglitz, J. (2006) Mid-Holocene El Niño-Southern Oscillation (ENSO) attenuation revealed by individual foraminifera in eastern tropical Pacific sediments. *Geology* **34**, 993–996.

- Koutavas, A., Lynch-Stieglitz, J., Marchitto Jr., et al. (2002) El Niño-like pattern in ice age tropical Pacific sea surface temperature. *Science* **297**, 226–230.
- Koutavas, A. and Sachs, J.P. (2008) Northern timing of deglaciation in the eastern equatorial Pacific from alkenone paleothermometry. *Paleoceanography* **23**, PA4205, doi:10.1029/2008PA001593.
- Kuhlbrot, T., Griesel, A., Montoya, M., et al. (2007) On the driving processes of the Atlantic meridional overturning circulation. *Review of Geophysics* **45**, RG2001, doi:10.1029/2004RG000166.
- Laosuthi, T. and Selover, D.D. (2007) Does El Niño affect business cycles? *Eastern Economic Journal* **33**, 21–42.
- Latif, M., Anderson, D., Barnett, T., et al. (1998) A review of the predictability and prediction of ENSO. *Journal of Geophysical Research* **103**, 14375–14393.
- Latif, M., Sperber, K.R., Arblaster, J.M., et al. (2001) ENSIP: the El Niño simulations intercomparison project. *Climate Dynamics* **18**, 255–276.
- Lawrence, K.T., Liu, Z. and Herbert, T.D. (2006) Evolution of the Eastern Tropical Pacific through Plio-Pleistocene glaciation. *Science* **312**, 79–83.
- Lea, D., Pak, D.K. and Spero, H.J. (2000) Climate impact of late quaternary equatorial Pacific sea surface temperature variations. *Science* **289**, 1719–1724.
- Lea, D.W., Mashiotta, T.A. and Spero, H.J. (1999) Controls on magnesium and strontium uptake in planktonic foraminifera determined by live culturing. *Geochimica et Cosmochimica Acta* **63**, 2369–2379.
- Lea, D.W., Pak, D.K., Peterson, L.C. and Hughen, K.A. (2003) Synchronicity of tropical and high-latitude Atlantic temperatures over the last glacial termination. *Science* **301**, 1361–1364.
- Lea, D.W., Pak, D.K., Belanger, C.L., et al. (2006) Paleoclimate history of Galapagos surface waters over the last 135,000 yr. *Quaternary Science Reviews* **25**, 1152–1167.
- Leduc, G., Vidal, L., Tachikawa, K., et al. (2007) Moisture transport across Central America as a positive feedback on abrupt climate changes. *Nature* **445**, 908–911.
- Leduc, G., Vidal, L., Cartapanis, O. and Bard, E. (2009) Modes of eastern equatorial Pacific thermocline variability: implications for ENSO dynamics over the last glacial period. *Paleoceanography* **24**, PA001701.
- Liu, Z., Brady, E. and Lynch-Stieglitz, J. (2003) Global ocean response to orbital forcing in the Holocene. *Paleoceanography* **18**, 1041, doi:10.1029/2002PA000819.
- Liu, Z. and Herbert, T.D. (2004) High-latitude influence on the eastern equatorial Pacific climate in the early Pleistocene epoch. *Nature* **427**, 720–723.
- Locarnini, R.A., Mishonov, A.V., Antonov, J.I., et al. (2006) *World Ocean Atlas 2005*, Volume 1: temperature. Levitus, S. (ed.) NOAA Atlas NESDIS 61, U.S. Government Printing Office, Washington D.C., 182 pp.
- Lohmann, G. and Lorenz, S.J. (2000) On the hydrological cycle under paleoclimatic conditions as derived from AGCM simulations. *Journal of Geophysical Research* **105**, 17417–17436.
- Longhurst, A.R. (1967) Vertical distribution of zooplankton in relation to the eastern Pacific oxygen minimum. *Deep Sea Research and Oceanographic Abstracts* **14**, 51–63.
- Lopes dos Santos, R.A., Prange, M., Castañeda, I.S., et al. (2010) Glacial–interglacial variability in Atlantic meridional overturning circulation and thermocline adjustments in the tropical North Atlantic. *Earth and Planetary Science Letters* **300**, 407–414.
- Lorenz, S.J., Kim, J.H., Rimbu, N., et al. (2006) Orbitally driven insolation forcing on Holocene climate trends: evidence from alkenone data and climate modeling. *Paleoceanography* **21**, PA1002.
- Loubere, P., Richaud, M., Liu, Z. and Mekik, F. (2003) Oceanic conditions in the eastern equatorial Pacific during the onset of ENSO in the Holocene. *Quaternary Research* **60**, 142–148.
- Lowell, T.V., Fisher, T.G., Comer, G.C., et al. (2005) Testing the Lake Agassiz meltwater trigger for the Younger Dryas. *Eos* **86**, 365–373.
- Mann, M.E., Cane, M.A., Zebiak, S.E. and Clement, A.C. (2005) Volcanic and solar forcing of the tropical Pacific over the past 1000 years. *Journal of Climate* **18**, 447–456.
- Marchitto, T.M., Muscheler, R., Ortiz, J.D., et al. (2010) Dynamical response of the tropical Pacific ocean to solar forcing during the Early Holocene. *Science* **330**, 1378–1381.
- MARGO Project Members (2009) Constraints on the magnitude and patterns of ocean cooling at the Last Glacial Maximum. *Nature Geosciences* **2**, 127–132.
- Marlow, J.R., Lange, C.B., Wefer, G. and Rosell-Mele, A. (2000) Upwelling intensification as part of the Pliocene-Pleistocene climate transition. *Science* **290**, 2288–2291.
- Martinez, J.I., Mora, G. and Barrows, T.T. (2007) Paleooceanographic conditions in the western Caribbean Sea for the last 560 kyr as inferred from planktonic foraminifera. *Marine Micropaleontology* **64**, 177–188.
- Mashiotta, T.A., Lea, D.W. and Spero, H.J. (1999) Glacial/interglacial changes in subantarctic sea surface temperature and  $\delta^{18}\text{O}$ -water using foraminiferal Mg. *Earth and Planetary Science Letters* **170**, 417–432.

- Matei, D., Keenlyside, N.S., Latif, M. and Jungclaus, J. (2008) Subtropical forcing of tropical Pacific climate and decadal ENSO modulation. *Journal of Climate* **21**, 4691–4709.
- McCrea, J.M. (1950) On the isotopic chemistry of carbonates and a paleotemperature scale. *Journal of Chemical Physics* **18**, 849–857.
- McGlone, M.S., Kershaw, A.P. and Markgraf, V. (1992) El Niño/Southern Oscillation climatic variability in Australasian and South American paleoenvironmental records. In: Diaz, H.F. and Markgraf, V. (eds) *El Niño: Historical and Paleoclimatic Aspects of the Southern Oscillation*. Cambridge University Press, Cambridge, pp. 435–462.
- McGregor, H.V., Dupont, L., Stuut, J.-B.W. and Kuhlmann, H. (2009) Vegetation change, goats, and religion: a 2000-year history of land use in southern Morocco. *Quaternary Science Reviews* **28**, 1434–1448.
- McIntyre, A. and Molino, B. (1996) Forcing of Atlantic equatorial and subpolar millennial cycles by precession. *Science* **274**, 1867–1870.
- Medina-Elizalde, M. and Lea, D.W. (2005) The Mid-Pleistocene Transition in the tropical Pacific. *Science* **310**, 1009–1012.
- Meehl, G.A., Washington, W.M., Wigley, T.M.L., et al. (2003) Solar and greenhouse gas forcing and climate response in the twentieth century. *Journal of Climate* **16**, 426–444.
- Meehl, G.A., Arblaster, J.M. and Branstator, G. (2008) A coupled air-sea response mechanism to solar forcing in the Pacific region. *Journal of Climate* **21**, 2883–2897.
- Merkel, U., Prange, M. and Schulz, M. (2010) ENSO variability and teleconnections during glacial climates. *Quaternary Science Reviews* **29**, 86–100.
- Meyer, I., Davies, G.R. and Stuut, J.-B.W. (2011) Grain size control on Sr-Nd isotope provenance studies and impact on paleoclimate reconstructions: an example from deep-sea sediments offshore NW Africa. *Geochemistry Geophysics Geosystems* **12**, Q03005.
- Milankovitch, M.M. (1941) *Kanon der Erdbestrahlungen und seine Anwendung auf das Eiszeitenproblem* Belgrade. New English Translation, 1998, *Canon of Insolation and the Ice Age Problem*. With introduction and biographical essay by Nikola Pantic. 636 pp. ISBN 86-17-06619-9.
- Mitchell, T. and Wallace, J.M. (1992) The annual cycle in equatorial convection and sea surface temperature. *Journal of Climate* **5**, 1140–1156.
- Mix, A. (2006) Running hot and cold in the eastern equatorial Pacific. *Quaternary Science Reviews* **25**, 1147–1149.
- Mohtadi, M., Oppo, D. W., Steinke, S., et al. (2011) Glacial to Holocene swings of the Australian-Indonesian monsoon, *Nature Geoscience* **4**, 540–544.
- Moy, C.M., G.O. Seltzer, D.T. Rodbell, and D.M. Anderson (2002) Variability of El Niño/Southern Oscillation activity at millennial timescales during the Holocene epoch. *Nature* **420**, 162–165.
- Mulitza, S., Prange, M., Stuut, J.-B.W., et al. (2008) Sahel megadroughts triggered by glacial slowdowns of Atlantic meridional overturning. *Paleoceanography* **23** PA4206, doi:10.1029/2008PA001637.
- Mulitza, S., Heslop, D., Pittauerova, D., et al. (2010) Increase in African dust flux at the onset of commercial agriculture in the Sahel region. *Nature* **466**, 226–228.
- Müller, P.J., Kirst, G., Ruhland, G., et al. (1998) Calibration of the alkenone paleotemperature index UK'37 based on core tops from the eastern South Atlantic and the global ocean (60°N–60°S). *Geochimica et Cosmochimica Acta* **62**, 1757–1772.
- Nägler, T.F., Eisenhauer, A., Müller, A., et al. (2000) The  $\delta^{44}\text{Ca}$ -temperature calibration on fossil and cultured *Globigerinoides sacculifer*: new tool for reconstruction of past sea surface temperatures. *Geochemistry Geophysics Geosystems* **1**, 1052, doi:10.1029/2000GC000091.
- Niedermeyer, E.M., Prange, M., Mulitza, S., et al. (2009) Extratropical forcing of Sahel aridity during Heinrich stadials. *Geophysical Research Letters* **36**, L20707, doi:10.1029/2009GL039687.
- Núñez, L., Grosjean, M. and Cartajena, I. (2002) Human occupations and climate change in the Puna de Atacama, Chile. *Science* **298**, 821–824.
- Nürnberg, D., Bijma, J. and Hemleben, C. (1996) Assessing the reliability of magnesium in foraminiferal calcite as a proxy for water mass temperatures. *Geochimica et Cosmochimica Acta* **60**, 803–814.
- O'Neil, J.R., Clayton, R.N. and Mayeda, T.K. (1969) Oxygen isotope fractionation in divalent metal carbonates. *Journal of Chemistry and Physics* **51**, 5547–5558.
- Östlund, G. and Stuiver, M. (1980) GEOSECS Pacific radiocarbon. *Radiocarbon* **22**, 25–53.
- Otto-Bliesner, B.L., Brady, E.C., Shin, S.-I., et al. (2003) Modeling El Niño and its tropical teleconnections during the last glacial-interglacial cycle. *Geophysical Research Letters* **30**, No. 23, 2198, GL01853.
- Pahnke, K., Sachs, J.P., Keigwin, L., et al. (2007) Eastern tropical Pacific hydrologic changes during the past 27,000 years from D/H ratios in alkenones. *Paleoceanography* **22**, PA4214, doi:10.1029/2007PA001468.
- Paul, H.A. (2002) *Application of Novel Stable Isotope Methods to Reconstruct Paleoenvironments: Compound-Specific Hydro-*

- gen Isotopes and Pore-Water Oxygen Isotopes*. Naturwissenschaften. ETH, Zürich, p. 149.
- Peeters, F., Acheson, R., Brummer, G.-J.A., et al. (2004) Vigorous exchange between the Indian and Atlantic oceans at the end of the past five glacial periods. *Nature* **430**, 661–665.
- Peltier, W.R. and Solheim, L.P. (2004) The climate of the Earth at Last Glacial Maximum: statistical equilibrium state and a mode of internal variability, *Quaternary Science Reviews* **23**, 335–357.
- Pena, L.D., Cacho, I., Ferretti, P. and Hall M.A. (2008) El Niño-Southern Oscillation-like variability during glacial terminations and interlatitudinal teleconnections. *Paleoceanography* **23**, PA3101.
- Peterson, L.C., Haug, G.H., Hughen, K.A. and Rohl, U. (2000) Rapid changes in the hydrologic cycle of the tropical Atlantic during the last glacial. *Science* **290**, 1947–1951.
- Pflaumann, U., Sarnthein, M., Chapman, M., et al. (2003) Glacial North Atlantic: sea-surface conditions reconstructed by GLAMAP 2000. *Paleoceanography* **18**, 1065, doi:10.1029/2002PA000774.
- Philander, S.G. and Fedorov, A.V. (2003) Role of tropics in changing the response to Milankovich forcing some three million years ago. *Paleoceanography* **18**, 1045, doi:10.1029/2002PA000837.
- Pielke Jr., R.A. and Landsea, C.W. (1999) La Niña, El Niño, and Atlantic hurricane damages in the United States. *Bulletin of the American Meteorological Society* **80**, 2027–2033.
- Pinot, S., Ramstein, G., Harrison, S.P., et al. (1999) Tropical paleoclimates at the Last Glacial Maximum: comparison of Paleoclimate Modeling Intercomparison Project (PMIP) simulations and paleodata. *Climate Dynamics* **15**, 857–874.
- Pisias, N.G. and Mix, A.C. (1997) Spatial and temporal oceanographic variability of the eastern equatorial Pacific during the late Pleistocene: evidence from radiolaria microfossils. *Paleoceanography* **12**, 381–393.
- Prahl, F.G. and Wakeham, S.G. (1987) Calibration of unsaturation patterns in long-chain ketone compositions for paleotemperature assessment. *Nature* **330**, 367–369.
- Prahl, F.G., Mix, A.C. and Sparrow, M.A. (2006) Alkenone paleothermometry: biological lessons from marine sediment records off western South America. *Geochimica et Cosmochimica Acta* **70**, 101–117.
- Prange, M., Lohmann, G., Romanova, V. and Butzin, M. (2004) Modelling tempo-spatial signatures of Heinrich Events: influence of the climatic background state. *Quaternary Science Reviews* **23**, 521–527.
- Prange, M., Steph, S., Schulz, M. and Keigwin, L.D. (2010) Inferring moisture transport across Central America: can modern analogs of climate variability help reconcile paleosalinity records? *Quaternary Science Reviews* **29**, 1317–1321.
- Prell, W.L. (1982) Oxygen and carbon isotope stratigraphy for the Quaternary of Hole 502B: evidence for two modes of isotopic variability. *Initial Reports DSDP, Leg 68, Curacao to Guayaquil, 1979*, 455–464.
- Prell, W.L. and Kutzbach, J.E. (1992) Sensitivity of the Indian monsoon to forcing parameters and implications for its evolution. *Nature* **360**, 647–652.
- Prins, M.A. and Weltje, G.J. (1999) End-member modeling of siliciclastic grain-size distributions: the Late Quaternary record of eolian and fluvial sediment supply to the Arabian Sea and its paleoclimatic significance. In: Harbaugh, J., Watney, L., Rankey, G., Slingerland, R., et al. (eds), *Numerical Experiments in Stratigraphy: Recent Advances in Stratigraphic and Sedimentologic Computer Simulations*. SEPM Special Publication 62. Society for Sedimentary Geology, Tulsa, pp. 91–111.
- Quinn, T.M., Taylor, F.W. and Crowley, T.J. (2006) Coral-based climate variability in the Western Pacific Warm Pool since 1867. *Journal of Geophysical Research* **111**, C11006, doi:10.1029/2005JC003243.
- Raymo, M.E. and Nisancioglu, K. (2003) The 41 kyr world: Milankovitch's other unsolved mystery. *Paleoceanography* **18**, 1011, doi:10.1029/2002PA000791.
- Regenberg, M., Steph, S., Nürnberg, D., et al. (2009) Calibrating Mg/Ca ratios of multiple planktonic foraminiferal species with  $\delta^{18}\text{O}$  calcification temperatures: paleothermometry for the upper water column. *Earth and Planetary Science Letters* **278**, 324–336.
- Rein, B., Lückge, A., Reinhardt, L., et al. (2005) El Niño variability off Peru during the last 20,000 years. *Paleoceanography* **20**, PA4003, doi:10.1029/2004PA001099.
- Riedinger, M.A., Steinitz-Kannan, M., Last, W.M. and Brenner, M. (2002) A ~6100  $^{14}\text{C}$  yr record of El Niño activity from the Galápagos Islands. *Journal of Paleolimnology* **27**, 1–7.
- Rodbell, D.T., Seltzer, G.O., Anderson, D.M., et al. (1999) An 15,000-year record of El Niño-driven alluviation in Southwestern Ecuador. *Science* **283**, 516–520.
- Rodgers, K.B., Charbit, S., Kageyama, M., et al. (2004) Sensitivity of Northern Hemispheric continental ice sheets to tropical SST during deglaciation. *Geophysical Research Letters* **31**, L02206, doi:10.1029/2003GL018375.
- Rodgers, K.B., Lohmann, G., Lorenz, S., et al. (2003) A tropical mechanism for northern hemisphere deglaciation.

- tion. *Geochemistry Geophysics Geosystems* **4**, 1046, doi:10.1029/2003GC000508.
- Romanova, V., Prange, M. and Lohmann, G. (2004) Stability of the glacial thermohaline circulation and its dependence on the background hydrological cycle. *Climate Dynamics* **22**, 527–538.
- Rosenthal, Y. and Broccoli, A.J. (2004) In search of paleo-ENSO. *Science* **304**, 219–221.
- Rosenthal, Y., Oppo, D.W. and Linsley, B.K. (2003) The amplitude and phasing of climate change during the last deglaciation in the Sulu Sea, western equatorial Pacific. *Geophysical Research Letters* **30**, 1428–1431.
- Rozanski, K., Araguás-Araguás, L. and Gonfiantini, R. (1992) Relation between long-term trends of oxygen-18 isotope composition of precipitation and climate. *Science* **258**, 981–985.
- Ruddiman, W.F. (2006) Orbital changes and climate. *Quaternary Science Reviews* **25**, 3092–3112.
- Rühlemann, C., Mulitza, S., Lohmann, G., et al. (2004) Intermediate depth warming in the tropical Atlantic related to weakened thermohaline circulation: combining paleoclimate data and modeling results for the last deglaciation. *Paleoceanography* **19**, 1025, PA1025, doi:10.1029/2003PA000948.
- Rühlemann, C., Mulitza, S., Müller, P.J., et al. (1999) Warming of the tropical Atlantic Ocean and slowdown of thermohaline circulation during the last deglaciation. *Nature* **402**, 511–514.
- Saher, M., Jung, S.J.A., Elderfield, H., et al. (2007) Sea surface temperatures of the western Arabian Sea during the last deglaciation. *Paleoceanography* **22**, PA2208.
- Saji, N.H., Goswami, B.N., Vinayachandran, P.N., and Yamagata, T. (1999) A dipole mode in the tropical Indian Ocean. *Nature* **401**, 360–363.
- Sandweiss, D.H., Richardson III, J.B., Reitz, E.J., et al. (1996) Geoarchaeological evidence from Peru for a 5000 years B.P. onset of El Niño. *Science* **273**, 1531–1533.
- Sandweiss, D.H., Maasch, K.A., Burger, R.L., et al. (2001) Variation in Holocene El Niño frequencies: climate records and cultural consequences in ancient Peru. *Geology* **29**, 605–606.
- Schefuß, E., Damste, J.S.S. and Jansen, J.H.F. (2004) Forcing of tropical Atlantic sea surface temperatures during the mid-Pleistocene transition. *Paleoceanography* **19**, PA4029.
- Schmidt, G.A., Hoffman, G. and Thresher, D. (2001) Isotopic tracers in coupled models: a new paleo-tool. *PAGES News* **9**, 10–11.
- Schmidt, M.W., Spero, H.J. and Lea, D.W. (2004) Links between salinity variation in the Caribbean and North Atlantic thermohaline circulation. *Nature* **428**, 160–163.
- Schneider, N., Venzke, S., Miller, A.J., et al. (1999) Pacific thermocline bridge revisited. *Geophysical Research Letters* **26**, 1329–1332.
- Schouten, S., Hopmans, E.C., Schefuß, E. and Sinninghe Damste, J.S. (2002) Distributional variations in marine crenarchaeotal membrane lipids: a new tool for reconstructing ancient sea water temperatures? *Earth and Planetary Science Letters* **204**, 265–274.
- Schouten, S., Ossebaer, J., Schreiber, K., et al. (2006) The effect of temperature, salinity and growth rate on the stable hydrogen isotopic composition of long chain alkenones produced by *Emiliana huxleyi* and *Gephyrocapsa oceanica*. *Biogeosciences* **3**, 113–119.
- Schrag, D.P., Hampt, G. and Murray, D.W. (1996) Pore fluid constraints on the temperature and oxygen isotopic composition of the glacial ocean. *Science* **272**, 1930–1932.
- Schulz, H., von Rad, U. and Erlenkeuser, H. (1998) Correlation between Arabian Sea and Greenland climate oscillations of the past 110,000 years. *Nature* **393**, 54–57.
- Servain, J., Wainer, I., McCreary Jr., J.P. and Dessier, A. (1999) Relationship between the equatorial and meridional modes of climatic variability in the tropical Atlantic. *Geophysical Research Letters* **26**, 485–488.
- Shackleton, N. (1974) Attainment of isotopic equilibrium between ocean water and the benthonic foraminifera genus *Uvigerina*: isotopic changes in the ocean during the last glacial. *Colloques internationaux Centre national de la recherche scientifique (France)* **219**, 203–209.
- Shackleton, N.J. (1987) Oxygen isotopes, ice volume and sea level. *Quaternary Science Reviews* **6**, 183–190.
- Shackleton, N.J. and Opdyke, N.D. (1973) Oxygen isotope and palaeomagnetic stratigraphy of Equatorial Pacific core V28–238: oxygen isotope temperatures and ice volumes on a  $10^5$  year and  $10^6$  year scale. *Quaternary Research* **3**, 39–55.
- Shackleton, N.J., Berger, A. and Peltier, W.R. (1990) An alternative astronomical calibration of the Lower Pleistocene timescale based on ODP Site 677. *Transactions – Royal Society of Edinburgh: Earth Sciences* **81**, 251–261.
- Shulmeister, J. and Lees, B.G. (1995) Pollen evidence from tropical Australia for the onset of an ENSO-dominated climate at c. 4000 B.P. *The Holocene* **5**, 10–18.
- Stommel, H., Arons, A.B. and Blanchard, D. (1956) An oceanographical curiosity: the perpetual salt fountain. *Deep Sea Research (1953)* **3**, 152–153.

- Stott, L., Cannariato, K., Thunell, R., Haug, G.H., et al. (2004) Decline of surface temperature and salinity in the western tropical Pacific Ocean in the Holocene epoch. *Nature* **431**, 56–59.
- Stott, L., Poulsen, C., Lund, S. and Thunell, R. (2002) Super ENSO and global climate oscillations at millennial time scales. *Science* **297**, 222–226.
- Stott, L., Timmermann, A. and Thunell, R. (2007) Southern hemisphere and deep-sea warming led deglacial atmospheric CO<sub>2</sub> rise and tropical warming. *Science* **318**, 435–438.
- Stuut, J.-B.W. and Lamy, F. (2004) Climate variability at the southern boundaries of the Namib (southwestern Africa) and Atacama (northern Chile) coastal deserts during the last 120,000 yr. *Quaternary Research* **62**, 301–309.
- Stuut, J.-B.W., Prins, M.A., Schneider, R.R., et al. (2002) A 300-kyr record of aridity and wind strength in southwestern Africa: inferences from grain-size distributions of sediments on Walvis Ridge, SE Atlantic. *Marine Geology* **180**, 221–233.
- Stuut, J.-B.W., Crosta, X., Van der Borg, K. and Schneider, R.R. (2004) The relationship between Antarctic sea ice and South-western African climate during the Late Quaternary. *Geology* **32**, 909–912.
- Stuut, J.-B.W., Zabel, M., Rattmeyer, V., et al. (2005) Provenance of present-day eolian dust collected off NW Africa. *Journal of Geophysical Research* **110**, D04202, doi:10.1029/2004JD005161
- Stuut, J.-B.W., Kasten, S., Lamy, F. and Hebbeln, D. (2007) Sources and modes of terrigenous sediment input to the Chilean continental slope. *Quaternary International* **161**, 67–76.
- Timmermann, A., Oberhuber, J., Bacher, A., et al. (1999). Increased El Niño frequency in a climate model forced by future greenhouse warming. *Nature* **398**, 694–696.
- Timmermann, A., An, S.I., Krebs, U. and Goosse, H. (2005) ENSO suppression due to weakening of the North Atlantic thermohaline circulation. *Journal of Climate* **18**, 3122–3139.
- Timmermann, A., Okumura, Y., An S.-I., et al. (2007) The influence of a weakening of the Atlantic meridional overturning circulation on ENSO. *Journal of Climate* **20**, 4899–4919.
- Tjallingii, R., Claussen, M., Stuut, J.-B.W., et al. (2008) Coherent high- and low-latitude control of the north-west African hydrological balance. *Nature Geoscience* **1**, 670–675.
- Tomczak, M. and Godfrey, J.S. (2001) *Regional Oceanography: An Introduction*. Elsevier Science Ltd., Oxford, England. PDF version from 2001, based on original version published 1994.
- Trenberth, K.E. (1997) The definition of El Niño. *Bulletin of the American Meteorological Society* **78**, 2771–2777.
- Trenberth, K.E. and Hurrell, J.W. (1994) Decadal atmosphere-ocean variations in the Pacific. *Climate Dynamics* **9**, 303–319.
- Trenberth, K.E., Branstator, G.W., Karoly, D., et al. (1998) Progress during TOGA in understanding and modelling global teleconnections associated with tropical sea surface temperatures. *Journal of Geophysical Research* **103**, 14291–14324.
- Tribbia, J.J. (1991) The rudimentary theory of atmospheric teleconnections associated with ENSO. In: Glantz, M.H., Katz, R.W. and Nicholls, N. (eds), *Teleconnections Linking Worldwide Climate Anomalies*. Cambridge University Press, Cambridge, pp. 285–308.
- Tudhope, A.W., Chilcott, C.P., McCulloch, M.T., et al. (2001) Variability in the El Niño-Southern Oscillation through a glacial-interglacial cycle. *Science* **291**, 1511–1517.
- Turney, C.S.M., Kershaw, A.P., Clemens, S.C., et al. (2004) Millennial and orbital variations of El Niño/Southern Oscillation and high-latitude climate in the last glacial period. *Nature* **428**, 306–310.
- Tziperman, E. and Gildor, H. (2003) On the mid-Pleistocene transition to 100-kyr glacial cycles and the asymmetry between glaciation and deglaciation times. *Paleoceanography* **18**, 1001, doi:10.1029/2001PA000627.
- Urey, H.C. (1947) The thermodynamic properties of isotopic substances. *Journal of the Chemical Society*, 562–581.
- Van Oldenborgh, G.J., Philip, S.Y. and Collins, M. (2005) El Niño in a changing climate: a multi-model study. *Ocean Science* **1**, 81–95.
- Visser, K., Thunell, R. and Stott, L. (2003) Magnitude and timing of temperature change in the Indo-Pacific warm pool during deglaciation. *Nature* **421**, 152–155.
- Waelbroeck, C., Labeyrie, L., Michel, E., et al. (2002) Sea-level and deep water temperature changes derived from benthic foraminifera isotopic records. *Quaternary Science Reviews* **21**, 295–305.
- Wan, X., Chang, P., Saravanan, R., et al. (2009) On the interpretation of Caribbean paleo-temperature reconstructions during the Younger Dryas. *Geophysical Research Letters* **36**, L02701, doi:10.1029/2008GL035805.
- Wang, P., Clemens, S., Beaufort, L., et al. (2005) Evolution and variability of the Asian monsoon system: state of the art and outstanding issues. *Quaternary Science Reviews* **24**, 595–629.

- Webster, P.J., Moore, A.M., Loschnigg, J.P. and Leben, R.R. (1999) Coupled ocean-atmosphere dynamics in the Indian Ocean during 1997–1998. *Nature* **401**, 356–360.
- Weldeab, S., Schneider, R.R. and Kölling, M. (2006) Deglacial sea surface temperature and salinity increase in the western tropical Atlantic in synchrony with high latitude climate instabilities. *Earth and Planetary Science Letters* **241**, 699–706.
- Weltje, G. (1997) End-member modelling of compositional data: numerical-statistical algorithms for solving the explicit mixing problem. *Journal of Mathematical Geology* **29**, 503–549.
- Wüst, G. (1935) Schichtung und Zirkulation des Atlantischen Ozeans: Die Stratosphäre. *Wissenschaftliche Ergebnisse der Deutschen Atlantische Expedition des Forschungs- und Vermessungsschiffs Meteor 1925–1927 6 1*, 180 pp.
- Zarriess, M., Johnstone, H., Prange, M., et al. (2011) Bipolar seesaw in the northeastern tropical Atlantic during Heinrich stadials. *Geophysical Research Letters* **38**, L04706, doi:10.1029/2010GL046070.
- Zebiak, S.E. (1993) Air-sea interaction in the equatorial Atlantic region. *Journal of Climate* **6**, 1567–1586.
- Zheng, W., Braconnot, P., Guilyardi, E., et al. (2008) ENSO at 6ka and 21ka from ocean-atmosphere coupled simulations. *Climate Dynamics* **30**, 745–762.
- Zhou, G.-T. and Zheng, Y.-F. (2003) An experimental study of oxygen isotope fractionation between inorganically precipitated aragonite and water at low temperatures. *Geochimica et Cosmochimica Acta* **67**, 387–399.
- Zhu, P. and Macdougall, J.D. (1998) Calcium isotopes in the marine environment and the oceanic calcium cycle. *Geochimica et Cosmochimica Acta* **62**, 1691–1698.